Leg 196 Preliminary Report

Deformation and Fluid Flow Processes in the Nankai Trough Accretionary Prism: Logging While Drilling and Advanced CORKs

2 May–1 July 2001

Shipboard Scientific Party

Ocean Drilling Program
Texas A&M University
1000 Discovery Drive
College Station TX 77845-9547
USA

August 2001

PUBLISHER'S NOTES

This report was prepared from shipboard files by scientists who participated in the cruise. The report was assembled under time constraints and does not contain all works and findings that will appear in the *Initial Reports* of the ODP *Proceedings*. Reference to the whole or to part of this report should be made as follows:

Shipboard Scientific Party, 2001. Leg 196 Preliminary Report. *ODP Prelim. Rpt.,* 96 [Online]. Available from World Wide Web: <http://www-odp.tamu.edu/publications/prelim/196_prel/196PREL.PDF>. [Cited YYYY-MM-DD]

Distribution: Electronic copies of this series may be obtained from the Ocean Drilling Program's World Wide Web site at http://www-odp.tamu.edu/publications.

This publication was prepared by the Ocean Drilling Program, Texas A&M University, as an account of work performed under the international Ocean Drilling Program, which is managed by Joint Oceanographic Institutions, Inc., under contract with the National Science Foundation. Funding for the program is provided by the following agencies:

Australia/Canada/Chinese Taipei/Korea Consortium for Ocean Drilling
Deutsche Forschungsgemeinschaft (Germany)
European Science Foundation Consortium for Ocean Drilling (Belgium, Denmark, Finland, Iceland, Ireland, Italy, The Netherlands, Norway, Portugal, Spain, Sweden, and Switzerland)
Institut National des Sciences de l'Univers–Centre National de la Recherche Scientifique (INSU-CNRS; France)
Marine High-Technology Bureau of the State Science and Technology Commission of the People's Republic of China
National Science Foundation (United States)
Natural Environment Research Council (United Kingdom)
Ocean Research Institute of the University of Tokyo (Japan)

DISCLAIMER

The following scientists and engineers were aboard the *JOIDES Resolution* for Leg 196 of the Ocean Drilling Program:

Logging While Drilling (LWD) Activities
2–28 May 2001

Hitoshi Mikada
Co-Chief Scientist
Deep Sea Research Department
Japan Marine Science and Technology Center
2-15, Natsushima-cho, Yokosuka-shi
Kanagawa 237-0061
Japan
Work: (81) 468-67-3983
Fax: (81) 468-66-5541
mikada@jamstec.go.jp

J. Casey Moore
Co-Chief Scientist
Earth Sciences Department
University of California, Santa Cruz
Santa Cruz CA 95064
USA
Work: (831) 459-2574
Fax: (831) 459-3074
cmoore@es.ucsc.edu

Adam Klaus
Staff Scientist
Ocean Drilling Program
Texas A&M University
1000 Discovery Drive
College Station TX 77845-9547
USA
Work: (979) 845-3055
Fax: (979) 845-0876
aklaus@odpemail.tamu.edu

Nathan L. Bangs
LWD Specialist
Institute for Geophysics
Building 600
University of Texas at Austin
4412 Spicewood Springs Road
Austin TX 78759-8500
USA
Work: (512) 471-0424
Fax: (512) 475-6338
nathan@utig.ig.utexas.edu

Sylvain Bourlange
LWD Specialist
Laboratoire de Geologie
École Normale Supérieure
24 Rue Lhomond
75231 Paris Cedex 05
France
Work: (33) 144322702
Fax: (33) 144322253
bourlang@ens.fr

Julien Broilliard
LWD Specialist
Laboratoire de Tectonophysique
Université Montpellier II
Place Eugene Bataillon
34095 Montpellier
France
Work: (33) 4-67-14-93-11
Fax: (33) 4-67-14-93-08
julien.broilliard@dstu.univ-montp2.fr

Warner Brückmann
LWD Specialist
GEOMAR
Christian-Albrechts-Universität zu Kiel
Wischhofstrasse 1-3
Building 4
24148 Kiel
Germany
Work: (49) 431-600-2819
Fax: (49) 431-600-2941
wbrueckmann@geomar.de

David S. Goldberg
LWD Specialist
Borehole Research Group
Lamont-Doherty Earth Observatory
Route 9W
Palisades NY 10964
USA
Work: (914) 365-8674
Fax: (914) 365-3182
goldberg@ldeo.columbia.edu

Sean S. Gulick
LWD Specialist
Institute for Geophysics
University of Texas at Austin
4412 Spicewood Springs Road
Building 600
Austin TX 78759-8500
USA
Work: (512) 471-0462
Fax: (512) 475-6338
sean@ig.utexas.edu

Martin Bak Hansen
LWD Specialist
Department of Earth Sciences
Subdepartment of Marine Geology
University of Åarhus
CF Møllers Alle
Bygning 110
DK-8000 Åarhus C
Denmark
Work: (45) 89422536
Fax: (45) 89422525
geomar@geo.aau.dk

Nathan Hayward
LWD Specialist
Geological Survey of Canada (Atlantic)/Bedford Institute of Oceanography
Marine Regional Geoscience
PO Box 1006
Dartmouth NS B2Y 4A2
Canada
Work: (902) 426-5070
Fax: (902) 426-6152
hayward@agc.bio.ns.ca

Denise J. Hills
LWD Specialist
Department of Geology and Geophysics/SOEST
University of Hawaii at Manoa
1680 East West Road
Honolulu HI 96822
USA
Work: (808) 956-4776
Fax: (808) 956-5154
djhills@akule.soest.hawaii.edu

Sabine Hunze
LWD Specialist
Insitut Für Geowissenshaftliche Gemeinschaftsaufgaben
Stilleweg 2
30655 Hannover
Germany
Work: (49) 511-643-3494
Fax: (49) 511-643-3665
hunze@gga-hannover.de

Masanori Ienaga
LWD Specialist
Ocean Research Institute
University of Tokyo
1-15-1 Minamidai, Nakano
Tokyo 164-8639
Japan
Work: (81) 3-5351-6538
Fax: (81) 3-5351-6438
ienaga@ori.u-tokyo.ac.jp

Lisa McNeill
Structural Geologist
School of Ocean and Earth Sciences
University of Southampton
Southampton Oceanography Centre
Southampton S014 3ZH
United Kingdom
Work: (44) 23 8059 3640
Fax: (44) 23 8059 3059
lcmn@soc.soton.ac.uk

Ong Swee Hong
LWD Engineer
Schlumberger K.K. Nagaoka Branch
14-30, Hokuyo 2-chome, Nagaoka-shi
Niigata-ken 940-0871
Japan
Work: (81) 258-24-9600
Fax: (81) 258-24-9620
gary_ong@citandak.oilfield.slb.com

Sheila Peacock
LWD Specialist
School of Earth Sciences
University of Birmingham
Edgbaston
Birmingham B15 2TT
United Kingdom
Work: (44) 121-414-6162
Fax: (44) 121-414-4942
s.peacock@bham.ac.uk

Thomas L. Pettigrew
Development Engineer
Ocean Drilling Program
Texas A&M University
1000 Discovery Drive
College Station TX 77845-9547
USA
Work: (979) 845-2329
Fax: (979) 845-2308
pettigrew@odpemail.tamu.edu

Saneatsu Saito
Logging Staff Scientist
Ocean Research Institute
University of Tokyo
1-15-1 Minamidai, Nakano-ku
Tokyo 164
Japan
Work: (81) 3-5351-6559
Fax: (81) 3-5351-6438
saito@ori.u-tokyo.ac.jp

Nophawit Thaiprasert
LWD Engineer
Schlumberger K.K. Nagaoka Branch
14-30, Hokuyo 2-chome, Nagaoka-shi
Niigata-ken 940-0871
Japan
Work: (81) 258-24-9600
Fax: (81) 258-24-9620
nthaiprasert@slb.com

Harold J. Tobin
LWD Specialist
Department of Earth and Environmental Science
New Mexico Institute of Mining and Technology
Socorro NM 87801
USA
Work: (505) 835-5920
Fax: (505) 835-6436
tobin@nmt.edu

CirculationObviationRetrofitKit(CORK)Activities
28 May–1 July 2001

Keir Becker
Co-Chief Scientist
Rosenstiel School of Marine and Atmospheric Science
University of Miami
Division of Marine Geology and Geophysics
4600 Rickenbacker Causeway
Miami FL 33149-1098
USA
Work: (305) 361-4661
Fax: (305) 361-4632
kbecker@rsmas.miami.edu

Hitoshi Mikada
Co-Chief Scientist
Deep Sea Research Department
Japan Marine Science and Technology Center
2-15, Natsushima-cho, Yokosuka-shi
Kanagawa 237-0061
Japan
Work: (81) 468-67-3983
Fax: (81) 468-66-5541
mikada@jamstec.go.jp

Adam Klaus
Staff Scientist
Ocean Drilling Program
Texas A&M University
1000 Discovery Drive
College Station TX 77845-9547
USA
Work: (979) 845-3055
Fax: (979) 845-0876
aklaus@odpemail.tamu.edu

Gary L. Austin
CORK Specialist/Engineer
Scripps Institution of Oceanography
University of California, San Diego
291 Rosecrans Street
San Diego CA 92106
USA
Work: (858) 534-9885
Fax: (858) 534-5255
gary@mpl.ucsd.edu

Ernest Ray Corn
Umbilical Engineer
Cabett Services, Inc.
6827 Signat Drive
Houston TX 77041
USA
Work: (713) 849-9131
Fax: (713) 849-9629
rcorn@cabett.com

Earl E. Davis
CORK Scientist
Pacific Geoscience Centre
Geological Survey of Canada
PO Box 6000
9860 West Saanich Road
Sidney BC V8L 4B2
Canada
Work: (250) 363-6453
Fax: (250) 363-6565
davis@pgc.nrcan.gc.ca

Peter B. Flemings
LWD/CORK Specialist
Department of Geosciences
Pennsylvania State University
442 Deike Building
University Park PA 16802-2714
USA
Work: (814) 865-2309
Fax: (814) 863-8724
flemings@geosc.psu.edu

Hiroyasu Ishiguro
Seismometer Engineer
Japan Drilling Co., Ltd.
Nishi-azabu Annex
3-20-16 Nishi-azabu, Minata-ku
Tokyo 106-0031
Japan
Work: (81) 3-5411-9889
Fax: (81) 3-5411-9202
hishi@jdc.co.jp

Masataka Kinoshita
Thermistor Scientist
Japan Marine Science and Technology Center
2-15 Natsushima-cho, Yokosuka
Kanagawa 237-0061
Japan
Work: (81) 468-67-3847
Fax: (81) 468-67-5541
sawa@jamstec.go.jp

Robert D. Macdonald
CORK Specialist/Engineer
Pacific Geoscience Centre
Geological Survey of Canada
9860 West Saanich Road
Sidney BC V8L 4B2
Canada
Work: (250) 363-6420
Fax: (250) 363-6565
macdonald@pgc.nrcan.gc.ca

Shinichi Obana (Sailed 21 June–1 July 2001)
Thermistor Engineer
Oceanographic Division
OCC Corporation
2-1 Shibaura, 1-chome, Minato-ku
Tokyo 105-6791
Japan
Work: (81) 03-5441-6038
Fax: (81) 03-5441-6065
obana@occ.ne.jp

Thomas L. Pettigrew
Development Engineer
Ocean Drilling Program
Texas A&M University
1000 Discovery Drive
College Station TX 77845-9547
USA
Work: (979) 845-2329
Fax: (979) 845-2308
pettigrew@odpemail.tamu.edu

Saneatsu Saito
Logging Staff Scientist
Ocean Research Institute
University of Tokyo
1-15-1 Minamidai, Nakano-ku
Tokyo 164
Japan
Work: (81) 3-5351-6559
Fax: (81) 3-5351-6438
saito@ori.u-tokyo.ac.jp

Takao Sawa
Seismometer Engineer
Marine Technology Department
Japan Marine Science and Technology Center
2-15 Natsushima-cho, Yokosuka
Kanagawa 237-0061
Japan
Work: (81) 468-67-3732
Fax: (81) 468-67-0970
sawa@jamstec.go.jp

Hikaru Tsurumi (Sailed 21 June–1 July 2001)
Thermistor Engineer
Kaminokawa Plant
OCC Corporation
3967 Kaminokawa-machi-kamachi-gun
Tochigi 329-0611
Japan
Work: (81) 285-56-3311
Fax: (81) 285-56-0481

ABSTRACT

Leg 196 was the second of a two-leg program of coring, logging, and installing advanced circulation obviation retrofit kit (ACORK) long-term hydrogeological observatories in the Nankai Trough, the type example of a convergent margin accreting a thick section of clastic sediments. The two-leg program was built on results from Leg 131 and was designed to define the interrelationship of deformation, structure, and hydrogeology in the Nankai accretionary prism. Leg 196 focused on logging while drilling (LWD) and installation of ACORKs at two sites near the toe of the Nankai prism: Site 808, cored during Leg 131 at the deformation front, and Site 1173, cored during Leg 190 as a reference site ~12 km seaward.

At Hole 1173B we collected LWD data to basement at 737 meters below seafloor (mbsf). Here the LWD data verify a subtle porosity increase with depth from 122 to 340 mbsf, followed downhole by a sharp decrease in porosity and return to a normal consolidation trend. The sharp decrease in porosity correlated with the diagenetic transition from cristobalite to quartz and is marked by a strong seismic reflector that is reproduced well by a synthetic seismogram based on the LWD data. Resistivity-at-the bit (RAB) images of the borehole show no evidence of a propagating protodécollement but, rather, reveal a basinal state of stress dominated by steeply dipping fractures and normal faults of variable strike.

In Hole 808I we acquired LWD data to just below the décollement (1035 mbsf), where poor drilling conditions precluded further penetration. Here RAB images provide unparalleled structural and stratigraphic detail across the frontal thrust and décollement that indicate northwest-southeast shortening consistent with the seismic reflection data. RAB images also document borehole breakouts that show a northwest-southeast oriented maximum principal in situ stress direction, nearly parallel to the maximum principal stress direction inferred from microfaults in cores and from the plate convergence direction. Resistivity curves suggest that the frontal thrust zone has compacted, presumably due to faulting. In contrast, the resistivity data suggest that the décollement zone is dilated. These resistivity anomalies in the frontal thrust and décollement zones cannot be explained by variations in pore water composition and need to be verified by the density and porosity logs, after careful correction for borehole washouts.

In Hole 1173B, a four-packer, five-screen ACORK installation was successfully emplaced. It was configured for monitoring the hydrogeological state and processes in basement and the stratigraphic projection of the décollement in the Lower Shikoku Basin formation. The ACORK in Hole 808I was configured with two packers and six screens and was intended to penetrate just to the décollement, with an emphasis on determining the hydrogeological state and processes at the frontal thrust, a fractured zone ~160 m below the frontal thrust, and the décollement. Owing to extreme deterioration of drilling conditions and underreamer failure, actual penetration concluded ~36 m short of the goal, but the ACORK remains a viable installation.

INTRODUCTION

Subduction zones are characterized by the world's largest and potentially most catastrophic earthquakes (Kanamori, 1986). Moreover, these plate convergence zones return materials to the Earth's interior with chemical fluxes that may impact global geochemical budgets and influence climate (Plank et al., 1998). Subduction zones also are the location of the incipient stages of formation of convergent and collisional mountain belts (Moores and Twiss, 1995).

Recent studies of the processes occurring at subduction zones have established beyond doubt that fluids play a major role in the physical and chemical evolution of subduction zones and mountain belts (e.g., Carson et al., 1990; Henry et al., 1989; Kastner et al., 1991; Vrolijk et al., 1991; Fisher, 1996). When sediments resting on the incoming or subducting plate meet the overriding plate, they are, in part, scraped off and deformed and, in part, underthrust. During this deformation and burial, tectonic stresses lead to the expulsion of intergranular fluids through compaction (Bray and Karig, 1985), increased temperatures cause mineral dehydration (Moore and Vrolijk, 1992), and biological and thermal processes produce hydrocarbons from organic matter (Suess and Whiticar, 1989). To understand the processes of fluid production, transport, and rock response requires not only detailed spatial and subsurface sampling but also long-term observations in the subseafloor. Accordingly, Ocean Drilling Program (ODP) Leg 196 was designed to measure the in situ physical properties and provide long-term monitoring of the physical and chemical states of the initial deformation zone of the subduction zone off of southwest Japan.

Evaluation of this solid and fluid flow in the subduction system off southwest Japan involves outstanding questions that can be addressed by our logging and monitoring program in combination with the borehole coring results from Legs 131 (Hill, Taira, Firth, et al., 1993) and 190 (Moore, Taira, Klaus, et al., 2001). These questions include

1. What is the character of the faulted rock and associated fluids of the plate-boundary thrust fault, or décollement?
2. What is the porosity or fluid content of the incoming sediments, the accretionary prism, and underthrust sediments?
3. What is the relationship between porosity and seismic velocity?
4. How and why does pore pressure vary between structural environments?
5. What changes in physical properties (especially velocity) occur in association with diagenetic alterations of sediments (particularly methane hydrate occurrence)?
6. What is the relationship between deformational structures at core, log, and seismic scales, and what do they tell us about tectonic processes in the accretionary prism?

Addressing these questions will provide a clearer understanding of the issues of deformation and fluid flow during shallow subduction and the basis for predicting the behavior of these materials at seismogenic depths.

GEOLOGICAL AND GEOPHYSICAL SETTING

The Nankai subduction zone off of southwest Japan forms an “end-member” sediment-dominated accretionary prism. Here, a sedimentary section ~1 km thick (Figs. F1, F2) is accreted to or underthrust beneath the margin in the style of a fold and thrust belt (Moore et al., 2001). The Philippine Sea plate underthrusts the margin at a rate of ~4 cm/yr along an azimuth of ~325° (Seno, 1977) down an interface dipping 3°–7° (Kodaira et al., 2000), causing repeated great earthquakes (magnitudes >8) with an average recurrence interval of ~180 yr (Ando, 1975). Currently the margin is locked with little convergence between the Muroto Peninsula and the Philippine Sea plate (Mazzotti et al., 2000). The convergent margin of southwest Japan has a geologic record of accretion of deep sea deposits extending to at least the Cretaceous (Taira et al., 1988). However, rocks cored during Leg

190 (Fig. F2) and even those subducted to seismogenic depths entered the subduction zone no earlier than the Pliocene (Moore, Taira, Klaus, et al., 2001).

In the area of Leg 190/196 drilling or the Muroto Transect (Fig. F1), the basin to margin transition can be divided into the Shikoku Basin and overlying trench fill, the protothrust zone, the imbricate thrust zone, the frontal out-of-sequence thrust zone, the large thrust slice zone, and the landward-dipping reflector zone (Fig. F2). A condensed summary of these tectonic provinces from Moore et al. (2001) and Moore, Taira, Klaus, et al. (2001) follows.

The Philippine Sea plate entering the Nankai Trough along the Muroto Transect is near the axis of an extinct spreading center marked by the Kinan Seamounts (Okino et al., 1999). As documented at Site 1173, the 16-Ma oceanic crust of the Shikoku Basin is overlain by, successively, volcaniclastics, a middle Miocene to mid-Pliocene massive hemipelagite, an upper Pliocene to lower Pleistocene hemipelagite with tephra layers, and a Pleistocene turbidite to hemipelagite transition sequence and a Pleistocene to Holocene trench turbidite unit.

Entering the protothrust zone, the ~1-km-thick sedimentary section initially deforms above a décollement zone or detachment surface developed in the latest Miocene massive hemipelagite layer. The lower portion of this massive hemipelagite is underthrust along with underlying volcaniclastics and oceanic crust. Coring and seismic studies demonstrate that this initial deformation above the décollement zone consists of small thrust faults associated with subtle folding at seismic scales (Park et al., 2000) and development of minor faults at core scale (Moore, Taira, Klaus, et al., 2001; Morgan and Karig, 1995).

Major thrust faulting and growth of the accretionary prism initiate at the frontal thrust and continue upslope (Fig. F2). Immediately landward of the frontal thrust, the imbricate thrust zone consists of a series of well-developed seaward-vergent imbricate packets spaced several kilometers apart. The imbricate thrust zone is ~20 km wide; Site 808 penetrates its frontal thrust. Out-of-sequence thrusts overprint the imbricate thrusts, starting ~20 km landward of the deformation front. Farther landward from the deformation front, out-of-sequence thrusts cutting thick thrust packages define the large thrust slice zone. These out-of-sequence thrusts were probably initially imbricated from thick turbidite sands of the Shikoku Basin (Moore, Taira, Klaus, et al., 2001). The landward-dipping reflector zone upslope from the large thrust slice zone is less well imaged than more seaward portions of the prism. However, the landward-dipping reflectors probably represent thrust boundaries.

FLUID FLOW INDICATORS AND LEG 196 OBJECTIVES

The Leg 190/196 drilling area shows high heat flow because the Muroto Transect is located near the extension of a ridge on the Philippine Sea plate (represented by the Kinan Seamounts) that ceased spreading at only 15 Ma. Conductive heat flow values range from 180 mW/m^2 at Sites 1173 and 1174 (Shipboard Scientific Party, 2001a, 2001b) to 130 mW/m^2 at Site 808 (Shipboard Scientific Party, 1991). Heat flow values decrease rapidly upslope from the Nankai Trough, verifying the anomalously warm nature of the trench area (Yamano et al., 1992). The simple extrapolation of conductive heat flow with depth may overestimate temperature because of the potential of heat advection associated with fluid expulsion from the deforming sedimentary sequence. The temperatures at the top of oceanic crust at Sites 1173 and 808 were estimated at 110° and 120°C, respectively, by a conductive extrapolation of shallower measurements (Shipboard Scientific Party,

1991, 2001a). A less reliable extrapolation of only two very shallow data points at Site 1174 suggests a comparable basement temperature there (Shipboard Scientific Party, 2001b). Thus, the evidence indicates that basement temperatures exceed 100°C at Sites 1173, 1174, and 808. These high temperatures drive diagenetic reactions that significantly influence log response.

Both thermal and geochemical measurements suggest fluid flow through the sediments in the Leg 196 area, although its magnitude is controversial. The temperature of the updip limit of the seismogenic zone is estimated to be ~150°C and is predicted to occur ~50 km northwest of Site 1174 (Wang et al., 1995). This estimated temperature is not much more than the basement temperatures estimated at Sites 808 and 1174. The apparently limited change in temperature between the seismogenic zone and the trench may be caused by flow of fluid upward along the décollement zone or through the permeable upper basaltic basement (Fisher, 1998).

Landward of the deformation front, the décollement zone steps down through a water-rich massive hemipelagite below, suggesting that the décollement zone is being progressively dewatered with the fluid possibly being expelled seaward up the décollement zone (Park et al., 2000). The broad minimum in the pore water chloride profile obtained during Legs 131 and 190 at Sites 808 and 1174, extending from right above to well below the décollement, was probably produced by a combination of in situ clay dehydration and fluid migration from depth (Kastner et al., 1993; Shipboard Scientific Party, 2001b).

Overall, the magnitude and location of active fluid flow in this accretionary prism and the potential linkage to the Nankai seismogenic zone are not clearly defined. Our desire to investigate this system motivated the deployment of long-term hydrogeological and geochemical monitoring systems or advanced circulation obviation retrofit kits (ACORKs) during Leg 196. By sampling particular stratigraphic and structural intervals, the ACORKs will constrain fluid pressures and permeability and provide a time series of the fluid flow regime at the toe of the Nankai accretionary prism. Thus, our results may provide a better understanding of the linkage of near-surface conditions to those in the seismogenic zone, especially in the case of an earthquake rupturing the deeper levels of the décollement zone.

SITE SUMMARIES

Site 1173

We drilled Holes 1173B and 1173C (Table T1) to obtain logging-while-drilling (LWD) data at a reference site on the seaward flank of the Nankai Trough and to install an ACORK long-term subseafloor hydrological monitoring experiment (Figs. F1, F2, F3, F4, F5). These holes complement Hole 1173A, which was cored from the surface to basement during Leg 190. This site provides a basis for comparison of physical and chemical properties between the incoming undeformed sediments and rocks of the Shikoku Basin with deformed materials of the accretionary prism and underthrust sediments cored at sites landward of the deformation front.

Log Quality

At Site 1173, the LWD tools measured resistivity at the bit (RAB), sonic velocity, density, porosity, natural gamma ray production, and photoelectric effect from the seafloor to basaltic basement. Additionally, the tools provided estimates of hole size and borehole resistivity images. A measurement-while-drilling (MWD) system supplied information on weight on bit (WOB), torque,

heave, resistivity, density, and sonic velocity that was communicated to the surface and displayed instantaneously during drilling.

The overall quality of the LWD logs recorded in Holes 1173B and 1173C is excellent. The LWD logs generally agree with the more limited Hole 1173A wireline logs. In Holes 1173B and 1173C the drilling rate was maintained between 35 and 60 m/hr throughout the section, and all measurements were made within 1 hr of bit penetration. At least two depth points were measured in each 0.30-m interval. The caliper shows that the gap between the bit radius and the hole is <1 in throughout both holes, except for the uppermost 75 m of Hole 1173C where soft sediment washed out a gap of up to 2 in. Therefore, the density log over this shallowest 75-m interval is unreliable. This was the first use of the LWD sonic velocity (ISONIC) tool in such fine-grained unlithified sediment and its first use by ODP. Although the tool worked well, the processing of the waveforms was not straightforward and will have to be improved postcruise to yield reliable sonic data.

Logging Units and Lithology

Both visual and multivariate statistical analyses of the logs define five logging units that account for the lithologic variations observed in the cores.

A high variability in the differential caliper log and a large number of caliper values >1 in reflect bad borehole conditions during drilling of logging Unit 1 (0–122 meters below seafloor [mbsf]). This logging unit shows high neutron porosity and low density values with a high standard deviation. Some of these variations are real and reflect silt and sand turbidites of the outer trench wedge facies.

A significant decrease of resistivity, density, and gamma ray and increase of neutron porosity with depth show an abnormal compaction trend and define logging Unit 2 (122–340 mbsf). This logging unit correlates with lithologic Unit II (102–344 mbsf), which consists of hemipelagic mud with abundant interbeds of volcanic ash. The low density could be related to a cementation effect due to the formation of cristobalite. The logging Unit 2/3 boundary correlates with the diagenetic phase transition between cristobalite and quartz.

High gamma ray, density, and photoelectric effect log values that increase continuously with depth distinguish logging Unit 3 (340–698 mbsf). Resistivity and, less obviously, gamma ray logs show a cyclicity (480–700 mbsf) that reflects changes in lithology, which may in turn reflect an interbedding of coarser and finer grained sediments.

Logging Unit 4 (698–731 mbsf) is defined by broad variations in photoelectric effect, resistivity, neutron porosity, and gamma ray logs that correlate well with the presence of the volcaniclastic facies of lithologic Unit IV (688–724 mbsf).

Logging Unit 5 (731–735 mbsf) shows an abrupt increase of resistivity and decrease of gamma ray, which characterize the basaltic oceanic basement.

Structural Geology

Structural data determined from RAB images of medium focused resistivity (penetration depth = 7.6 cm) indicate sparse deformation and predominantly subhorizontal bedding dips. Increases in bedding dips (5°–35°) at 50–200 mbsf and below ~370 mbsf agree with core data from Hole 1173A. Fractures are high angle (40°–80°), show normal displacement where measurable, and have random orientation. An increase in fracture intensity occurs at 380–520 mbsf, correlating with increased bedding dip. The upper limit of this zone corresponds to the projected stratigraphic equivalent of the décollement. At ~500 mbsf, bands of heterogeneous (mottled) high resistivity probably represent

zones of intense deformation or brecciation. In general, deformation observed in Holes 1173B and 1173C is consistent with extensional faulting probably related to basinal compaction and burial and not propagating compressional deformation from the accretionary wedge.

Physical Properties

LWD density data in Holes 1173B and 1173C closely match core physical properties data from Hole 1173A, except for the uppermost 60 mbsf, where differential caliper exceeded 1 in. LWD densities are nearly constant in logging Subunit 1b (55–122 mbsf) and logging Unit 2 (122–340 mbsf), with the notable exceptions of two high-amplitude variations near the transition from logging Unit 2 (Upper Shikoku Basin) to lithologic Unit III (Lower Shikoku Basin). Logging Unit 3 (340–698 mbsf) is characterized by a steady increase in density consistent with a normal compaction trend. The LWD resistivity logs clearly respond to the lithologic boundaries identified in Hole 1173A. Within logging Unit 2 resistivity decreases with depth, whereas, in logging Unit 3, resistivity is nearly constant with depth, in contrast to the behavior of density in these two units. All LWD resistivity logs show similar overall resistivity trends, in good agreement with available wireline logs. Shallow button resistivities that are consistently higher than medium and deep resistivities are unusual and an unexplained feature of the Site 1173 LWD data.

Logs and Seismic Reflection Data

The velocities from the core and wireline data and densities from the core and LWD data from 0 to 350 mbsf were used to generate a synthetic seismogram in good agreement with the seismic reflection data. Good correlations exist between the synthetic seismogram and seismic reflections at ~80–100 (trench–basin transition facies), ~175, ~265–270, and ~300–350 mbsf (associated with the Upper/Lower Shikoku Basin unit boundary and the logging Unit 2/3 boundary). An increase in acoustic impedance associated with the phase transition from cristobalite to quartz may be, in part, responsible for this reflection. High reflectivity in the synthetic seismogram beneath ~350 mbsf does not match with the low reflectivity in the seismic data of the Lower Shikoku Basin unit (logging Unit 3) and may be due to a sampling bias toward more cohesive, higher velocity samples in the core velocity measurements.

ACORK Installation and Basement Coring

A four-packer, five-screen, 728-m-long ACORK string (Fig. F5) was deployed through the sediment section in Hole 1173B, configured to emphasize long-term observations of pressures in three principal zones, as follows:

1. Oceanic basement below 731 mbsf, to determine permeability and pressures in the young oceanic crust being subducted and thereby assess the role of oceanic crust in the overall hydrogeology at Nankai Trough. A screen was installed immediately above the ACORK shoe, centered at 722 mbsf, and a packer was placed immediately above the screen.
2. Lower Shikoku Basin formation, well below the stratigraphic projection of the décollement, to assess the hydrological properties of a reference section of the Lower Shikoku formation and test for fluid pressure propagation from basement or possibly higher in the section. A packer was centered at 495 mbsf to isolate a screen centered at 563 mbsf.

3. The predécollement or stratigraphic projection of décollement at ~390–420 mbsf in the upper part of the Lower Shikoku formation seaward from Sites 1174 and 808. A symmetric array, ~100 m long, comprising three screens separated by two packers, was built into the ACORK string so that the screens were centered at 439, 396, and 353 mbsf. Objectives of this array include (a) documenting the variation of hydrogeological properties across and away from this zone as a reference for the state of the formation before the décollement actually develops closer to the trench axis and (b) detecting the possibility of fluid flow along the stratigraphic projection of the décollement. In addition, the central screen in this array (the screen that spans the predécollement) includes a second small-diameter line for eventual sampling of formation fluids from the well head.

After ACORK installation, the rotary core barrel (RCB) coring bottom-hole assembly (BHA) was successfully deployed through the ACORK casing to deepen the hole into basement to assure that the signal of basement hydrogeological processes will be transmitted to the deepest screen. A total of 19.5 m into basement was cored, with recovery of 5.2 m (27% recovery). The core comprises basaltic basement overlain by a thin veneer of volcaniclastics.

Following the basement coring, the final step in the ACORK installation at Hole 1173B was deployment of a bridge plug to seal the bore of the casing and isolate the basement section to be monitored by the deepest screen. We intended to set the bridge plug very near the bottom of the ACORK string, allowing future deployment of other sensor strings within the central bore. However, the bridge plug apparently set prematurely at 466 mbsf; this was not sensed at the rig floor and ensuing operations resulted in breaking the pipe off at the ACORK head. Nevertheless, detailed analysis suggests that the bridge plug is indeed set and there should be no broken pipe outside the ACORK head to inhibit future data recovery operations.

Site 808

We drilled Hole 808I (Table T1) to obtain LWD data through the frontal thrust zone and décollement zone at the deformation front of the Nankai Trough and to install an ACORK long-term subseafloor hydrological monitoring experiment (Fig. F6). This hole complements cores recovered at Site 808 during Leg 131. Coring, logging, and monitoring here are intended to document the physical and chemical state of the Nankai accretionary prism and underthrust sediments through the frontal thrust zone, the décollement zone, and into oceanic basement.

Log Quality

The overall quality of the LWD logs recorded in Hole 808I is variable. We recorded at least one sample per 15 cm over 99% of the total section. Sections of enlarged borehole estimated by the differential caliper yield unreliable density data and associated derived porosity that is confirmed by comparison to core data. This problem is primarily associated with the depth intervals of 725–776 and 967–1057 mbsf, in which there was a long duration between drilling and recording of the logs due to wiper trips or poor hole conditions. Density and density-derived porosity should be used cautiously until more complete corrections and editing are completed postcruise. Although the LWD ISONIC tool worked well, the processing of the waveforms was not straightforward and postcruise processing is required to yield reliable sonic data.

Logging Units and Lithology

A combination of visual interpretation and multivariate statistical analysis defined four logging units and six subunits.

Logging Unit 1 (156–268 mbsf) is characterized by the overall lowest mean values of gamma ray, density, and photoelectric effect and overall highest mean values of resistivity and neutron porosity. These values coincide with very fine grained sandstone, siltstone, and clayey siltstone/silty claystone observed in the cores.

Logging Unit 2 (268–530 mbsf) shows a constant value range of gamma ray and neutron porosity and a decreasing resistivity log. A high variability in differential caliper log and a large number of values >1 in reflect poor borehole conditions.

Logging Unit 3 (530–620 mbsf) is marked by a significant increase of the mean values of gamma ray, density, and photoelectric effect logs.

Logging Unit 4 (620–1035 mbsf) is characterized by the overall highest mean values of gamma ray, photoelectric effect, and density and the lowest mean values of resistivity and neutron porosity. Generally, a positive correlation between gamma ray and photoelectric effect is observed.

A continuous increase in gamma ray and photoelectric effect, which reflects an increase in clay and carbonate content, is observed from logging Unit 1 to logging Unit 4. A positive correlation of resistivity with density defines logging Units 3 and 4.

Structural Geology

RAB tools imaged fracture populations and borehole breakouts throughout much of the borehole. We identified both resistive and conductive fractures, respectively interpreted as compactively deformed fractures and open fractures. Fractures are concentrated in discrete deformation zones that correlate with core analysis of Leg 131 Site 808: the frontal thrust zone (389–414 mbsf), a fractured interval (559–574 mbsf), and the décollement zone (~940–960 mbsf). Only relatively sparse deformation occurs between these zones. Fractures are steeply dipping (majority >30°) and strike predominantly east-northeast–west-southwest, close to perpendicular to the convergence vector (~310°). Bedding dips are predominantly low angle (<50°) but are difficult to identify in the highly deformed zones, therefore biasing this result. Bedding strike is more random than fracture orientation, but, where a preferred orientation is recorded, beds strike subparallel to fractures and perpendicular to the estimated convergence vector.

The frontal thrust zone (389–414 mbsf) represents the most highly deformed zone in Hole 808I and contains predominantly S-dipping fractures (antithetic to the seismically imaged main thrust fault) and a few north-dipping east-northeast–west-southwest striking fractures. The highly fractured interval at 559–574 mbsf contains similar fracture patterns to the frontal thrust zone. Both deformation zones are characterized by high-conductivity (open?) fractures within a zone of overall high resistivity.

Deformation close to the décollement is more subdued and is represented by a series of discrete fracture zones. The décollement in the RAB images (937–965 mbsf) is defined by a general increase in fracture density and variability in physical properties.

Borehole breakouts are recorded throughout Hole 808I and are particularly strongly developed within logging Unit 2 (270–530 mbsf), suggesting lithologic control on sediment strength and breakout formation. Breakouts indicate a northeast-southwest orientation for the minimum horizontal compressive stress (σ_2), consistent with a northwest-southeast convergence vector (310°,

parallel to σ_1). Breakout orientation deviates slightly from the dominant strike of fractures (east-northeast–west-southwest), but this deviation may be within error of measurements.

Physical Properties

The Hole 808I LWD density log shows a good fit to the core bulk density, slightly underestimating core values in the upper 550 mbsf and slightly overestimating core values between 550 and 970 mbsf. Below 156 mbsf the LWD density log shows a steady increase from ~1.7 to ~1.95 g/cm^3 at 389 mbsf. Between 390 and 415 mbsf density varies greatly, corresponding to the frontal thrust zone. Below the frontal thrust zone density decreases sharply to ~1.85 g/cm^3. Below 530 mbsf it increases to ~2.1 g/cm^3. Between 725 and 776 mbsf density drops sharply to ~1.75 g/cm^3, corresponding to a period of borehole wiper trips. Density increases more rapidly from ~1.95 g/cm^3 at 776 mbsf to 2.25 g/cm^3 at 930 mbsf, decreasing steadily to ~2.15 g/cm^3 before stepping down to 1.4 g/cm^3 at 965 mbsf. This corresponds to the base of the décollement zone; below, density increases steadily from ~1.7 g/cm^3 at 975 mbsf to ~2.0 g/cm^3 at 1034.79 mbsf.

The downhole variation of LWD resistivity measurements shows identical trends in all five Hole 808I resistivity logs; all logging unit boundaries are clearly identified. Logging Unit 1 has an average resistivity of ~0.8–0.9 Ωm. After a sharp decrease in resistivity from 1.3 to 0.5 Ωm between 156 and 168 mbsf, the signal shows an increasing trend downward to the boundary between logging Units 1 and 2. Logging Unit 2 is characterized by an overall decreasing trend in resistivity from ~0.9 to ~0.6 Ωm. However, this trend is sharply offset from 389 to 415 mbsf (logging Subunit 2b), where the resistivity values are ~0.3 Ωm higher. This zone seems to correspond to the frontal thrust; the higher resistivity here may reflect compactive deformation in the frontal thrust zone. Logging Unit 3 shows a higher degree in variability of the resistivity signal. Resistivity exhibits less variation again in logging Unit 4, where it averages ~0.6 Ωm. As observed in Hole 1173B, shallow resistivity is systematically higher than both medium and deep resistivity.

Logs and Seismic Reflection Data

Beneath the depth of the casing (~150 mbsf), correlations between the synthetic seismogram and seismic reflection data are only broadly consistent and the defined lithologic boundaries or units correlate at some depth intervals. The details of amplitude and waveform throughout most of the section do not match the seismic data. Amplitudes of the intervals between ~200 and ~400 mbsf, between ~750 and ~850 mbsf, and below ~925 mbsf are significantly higher in the synthetic seismogram than in the seismic data and are probably generated by numerous anomalously low velocity and density values, which are a product of poor hole conditions.

ACORK Installation

In Hole 808I we assembled a 964-m-long ACORK casing string incorporating two packers and six screens for long-term observations of pressures in three principal zones, as follows:

1. The décollement and overlying section of the Lower Shikoku Basin (lithologic Unit IV). A screen was placed immediately above the casing shoe, with a packer immediately above the screen. The hole was opened with the intent of emplacing the screen just into the décollement, with the packer positioned in a competent zone immediately above the décollement. Three other screens were configured above the packer, to span the upper section

of the Lower Shikoku formation to study the variation of physical properties and the propagation of any pressure signals away from the décollement.
2. A fractured interval at 560–574 mbsf in the Upper Shikoku Basin formation, as identified in RAB logs (see "Structural Geology"). A single screen was intended to be deployed in this zone.
3. The frontal thrust, centered at ~400 mbsf. A single screen was intended to be deployed in this zone.

Drilling conditions during installation of the ACORK steadily worsened, starting ~200 m above the intended depth. Despite all efforts, progress stopped 37 m short of the intended installation depth. This left the screen sections offset above the intended zones (Fig. F6), not an ideal installation but still viable in terms of scientific objectives. In addition, this left the ACORK head 42 m above seafloor, unable to support its own weight once we pulled out. Fortunately, when the ACORK head fell over, it landed on the seafloor such that all critical components remained in good condition. This includes the critical hydraulic umbilical, data logger, and the underwater-mateable connector, which remains easily accessible by a remotely operated vehicle (ROV) or by submersible for data download.

TOPICAL HIGHLIGHTS AND QUESTIONS

Borehole Images, Structural Characterization, Breakouts, Stress Orientations, and Stress Magnitudes

Imaging of the borehole by RAB provided one of the immediate products of Leg 196 (Figs. F7, F8). The RAB images provide an in situ image of borehole structure unparalleled in completeness, although at a lower resolution than the cores. Nevertheless, combining these images with information on core structures provides probably the best view so far of the initial deformation in a subduction zone. At Site 1173 we imaged steeply dipping normal faults and fractures of variable strikes, which would be expected from the state of stress in a consolidating sedimentary basin. Conversely, the fractures are more consistent in dip azimuth in Hole 808I (Fig. F7), suggesting an influence of the compressional deformation at the frontal thrust. One of the most spectacular results of Leg 196 is imaging the breakouts in Hole 808I and their definition of a principal stress orientation parallel to that determined by the inversion of small faults (Lallemant et al., 1993) and parallel to that expected from the convergence vector (Seno et al., 1993). These breakouts are concentrated in lithologic Subunit IIC at Site 808. Additional analysis of breakout orientation, width, and depth along with determination of the cohesion and coefficient of friction of the sedimentary rocks should provide a better resolution of stress orientation as well as stress magnitude.

Contrasting Log Response across Faults and Predictions of Fluid Pressure

Tectonic consolidation of sediment in fault zones is influenced by fluid pressure. Thus, depth profiles of density or porosity variation through fault zones provides an overall view of fault zone behavior and a qualitative predictor of fluid pressure. From Hole 808I, we collected log data through the frontal thrust and décollement zones. This information, combined with existing core-scale density and porosity information, provides a unique view of major fault dynamics.

The density and density-derived porosity logs are suspect in the frontal thrust and décollement zones because of enlarged hole diameter. However, resistivity data provide insights on porosity variation. For example, the frontal thrust zone shows a sharp and sustained increase in resistivity.

Because the pore water shows no significant variations in composition through this zone, it is unlikely that the resistivity increase is caused by differing fluid composition. Rather, the increase in resistivity may indicate a densification of the rock unit due to compaction accompanying shear.

At the top of the décollement zone, the resistivity trend changes from gradually increasing to gradually decreasing. The pore water chemistry around the décollement zone shows no anomalies that would explain the decreasing resistivity. The decreasing resistivity trend is presumably a response to the increased amount of fluid-filled unhealed fractures and a bulk porosity increase. In contrast, core porosity decreases in the décollement zone. Therefore, a combination of log and core measurements suggests that the décollement is an interval of enhanced porosity (probably fracture porosity) that encompasses blocks of sediment of relatively lower porosity and high density. Thus, the log data suggest that the fracture porosity of the décollement zone is dilated, probably held open by high fluid pressure, in contrast to the frontal thrust zone that is densified and may not be currently as highly overpressured.

The interpretations of fault zone porosity based on qualitative interpretation of resistivity must be verified by calculation of resistivity-derived porosity and appropriate corrections to the density data so that they can be utilized to calculate porosity. Additionally, direct fluid pressure measurements from the ACORK installation may provide information on fault zone pore pressures.

Porosity Changes, Silica Diagenesis, Reflectors, and the Décollement Zone

At Site 1173 density and porosity change downsection atypically for a normally consolidating sedimentary basin (Fig. F5). After remaining constant for ~200 m above, the porosity decreases sharply at ~340 mbsf and follows a normal consolidation curve below (Shipboard Scientific Party, 2001a). The porosity decrease at ~340 mbsf is associated with a diagenetic shift from cristobalite to quartz (Shipboard Scientific Party, 2001a), probably due to the alteration of vitric volcanic ash (Tada and Iijima, 1983) and siliceous microfossils. The stepwise porosity reduction at the cristobalite–quartz transition at Site 1173 mimics similar sharp porosity reductions across a similar phase transition (opal-CT to quartz) in siliceous rocks (Isaacs et al., 1983). Isaacs et al. (1983) believe that the opal-CT to quartz transition is associated with a reorganization and partial collapse of the sediment fabric that had previously been held open by an opal-CT cementation effect. A similar process could explain the sharp shift in porosity at Site 1173. At Site 1173 the abrupt shift in porosity and density at 320 to 360 mbsf generates a strong seismic reflection. This reflection cuts upsection across stratigraphy from southeast of Site 1173 northwesterly toward the margin (Fig. F4). An important question is, "What is the three-dimensional geometry of this reflector?"

The cristobalite to quartz phase transition occurs above the stratigraphic level to which the déollement would project at Site 1173, also at Site 1174, and, arguably, at Site 1177. Thus, the décollement seems to propagate seaward entirely in the apparently stronger, more dewatered portion of the Shikoku Basin formation and does not jump upsection to the less-dewatered section above 320 mbsf. Key questions raised by this observation are, "What is the real strength difference between the sediments above and below the cristobalite to quartz phase transition?" and "What is its effect on décollement development?"

ISONIC Velocity Data

For the first time in ODP history, LWD sonic velocity data were recorded during Leg 196 using the Schlumberger ISONIC tool. In situ velocity information is a key measurement because velocity is the

fundamental link between seismic imaging and geology and because velocity is highly sensitive to stress, limiting the utility of shipboard core sample measurements. ISONIC data were recorded at both Sites 1173 and 808. Owing to the complex signal arrivals and the variety of phases propagating along the tool, picking compressional wave traveltimes (and, hence, velocity) is not straightforward. Initial traveltime analysis of the waveforms recorded during the leg did not produce reliable velocity values, although features in the velocity logs broadly correlate with those in the resistivity and density logs. Usable velocity and acoustic impedance results will require detailed waveform analysis to be carried out postcruise.

OPERATIONS SYNOPSIS

Keelung Port Call

Leg 196 began with the first line ashore to Berth 4-E East Wharf, Keelung, Taiwan, at 0904 hr on 2 May 2001. Public relations tours were held each day with members of the press. VIP tours (including the Taiwanese vice president) were conducted on 4 May, and the bulk of the visitors were on board on 5 and 6 May. Major port call activities consisted of removing geochemical radioactive sources from the ship and loading a considerable amount of equipment, including ACORK casing (260 joints) and hardware, the Anadrill LWD and MWD tools, and 120 tons of sepiolite.

Immigration formalities were completed on 2 May, and the loading of 700.0 metric tons of fuel from 100 metric ton barges was finished at 2050 hr. Divers inspected the thrusters and main propulsion system to ensure they were not fouled by fishing lines during Leg 195. Additional inspection dives were conducted on the afternoon of 3 May.

On 3 May the vessel was shifted 40 ft astern to make room for other ships berthing at the dock; the incoming air freight and food were loaded. We then unloaded surface freight containers, placed the freight onto the dock, and began loading it onto the ship. The Anadrill MWD/LWD tools were unloaded onto the dock, and the Anadrill engineers began dockside assembly and testing. The loading of the bulk sepiolite began, using a pneumatic truck to transfer it onto the ship; 56 tons was loaded. Liquid helium was received, and the cryogenic magnetometer was filled.

After considerable efforts to coordinate logistics and obtain permits, the two radioactive sources for the geochemical logging tool were taken off the drillship on 4 May. Then we were allowed to load the sources for the LWD/MWD logging tools onto the ship. On 4 May the Anadrill engineers continued unloading and testing the LWD/MWD tools, and the remaining 64 short tons of bulk sepiolite was loaded. The trucks carrying the 10.75-in and 20-in casing began arriving, and we started to unload and stage it on the dock; during this process each joint was measured and labeled.

On 5 May, assembly and testing of the LWD/MWD tools continued, the casing handling and loading continued, and the off-going freight was taken off the ship. By 0830 hr on 6 May all casing had been loaded. A total of 226 joints of 10.75-in casing was stored in the riser hold, and 36 joints of 20-in casing was stored in the riser hold, as well as on top of the riser hold hatch, as the riser hold was full. The LWD/MWD tool testing was completed, the tools loaded, and the crew began securing the ship for departure.

Transit from Keelung, Taiwan, to Site 1173

The last line away from Keelung was at 0900 hr on 7 May. The transit to Site 1173 began at 0930 hr when the harbor pilot was disembarked. After a transit of 784 nmi we arrived at the Global

Positioning System (GPS) coordinates of Site 1173 (32˚14.6634′N, 135°1.5085′E) at 0645 hr on 10 May.

During the transit, the rig crew assembled the first reentry cone; it was moved into position on the moonpool doors in preparation for deployment. Repairs were made to the underreamer used during Leg 195 (seal replacements, 22-in cutter sets changed, and jet function verified). The rig crew performed preventive rig maintenance and repairs.

The ship experienced a power interruption during the transit (at 2347 hr on 8 May) caused by a shutdown of main engine #2 due to high crank-case pressure. This resulted in a slight reduction in speed that lasted 15 min. Repairs to the piston pin and insert carrier on cylinder #7 were made, and complete preventive maintenance was performed on this engine.

In preparation for operations at Site 1173, we attached a used 18.5-in tricone mill-tooth bit (Hughes X44) to the 22-in underreamer. This, in turn, was made up to an 8.25-in positive displacement mud motor (Baker-Hughes Drilex model D825MSHF), and the assembly was tested. The pressure drop at a flow rate of 275 gallons per minute (gpm) was low (75 psi) and leakage high, so we changed to a backup mud motor that had a 125-psi pressure drop at 275 gpm. The Dril-Quip cam-actuated drill-ahead (DQ CADA) casing running tool was made up to the 20-in casing hanger and a short (pup) joint of casing.

Site 1173

Hole 1173B

At 0645 hr on 10 May we arrived on location, lowered the thrusters and hydrophones, and started making up five stands of drill collars. A positioning beacon was not immediately deployed because the scientists requested an offset of 50 m at 314° from the position of Hole 1173A, which was cored during Leg 190; the ship maintained station by using the GPS. The ship was over the desired position of Hole 1173B at 0810 hr on 10 May, and a seafloor positioning beacon (Datasonics SN2031, 14.0 kHz, 214 dB) was deployed at 0835 hr.

Reentry Cone and Casing Operations

At 1200 hr on 10 May, we began rigging up to run 20-in casing by welding a casing guide shoe to the bottom joint and then adding nine more joints of casing. This casing was then added to the short (pup) joint of 20-in casing attached to the bottom of the casing hanger that was already latched to the casing running tool; the total length of this assembly was 120.6 m. This assembly was then landed and latched into the reentry cone at 1845 hr; the running tool was unlatched so that the BHA could be run into the casing.

Next, we began assembling and running the drilling BHA into the casing. The BHA consisted of the 18.5-in bit, 22-in underreamer, bit sub with float, mud motor, and four stands of 8.25-in drill collars for a total length of 123.5 m. The casing running tool was attached to the top of the BHA; the BHA was lowered into and latched to the casing and reentry cone. The reentry cone, BHA, and casing were lowered through the moonpool at 2100 hr.

By 0800 hr on 11 May, we had lowered 4781.77 m of drill string and deployed the vibration-isolated television (VIT) camera in preparation for spudding Hole 1173B. A backup seafloor positioning beacon (Datasonics SN2029; 15.0 kHz; 214 dB) was deployed at 0635 hr. When the VIT camera reached the casing running tool at 1030 hr, we observed that the reentry cone was missing

but that the running tool and casing hanger were still attached to the drill string. We began assembling the second reentry cone.

The VIT camera was recovered; we changed the VIT camera drill pipe guide sleeve with the larger casing guide sleeve so we could lower the camera over the casing to inspect it. At 1515 hr, the camera was lowered over the running tool, and we began inspecting the casing. The entire casing string, bit, and underreamer appeared to be intact. We continued to the seafloor with the drill string and camera to see if we could locate the lost reentry cone. We were unable to locate the reentry cone; the search was abandoned at 1930 hr; we began tripping out of the hole so we could rig up the second reentry cone.

On 12 May, we had raised the drill pipe, secured the casing in the moonpool, removed the casing running tool, racked the drill collars in the derrick, and laid down the mud motor, underreamer, and bit. At this time we had to perform the routine slipping and cutting of the drill line, which was completed at 1100 hr. The casing was taken apart at the first collar, and the second reentry cone was moved into position over the casing collar. The top piece of casing was reattached through the reentry cone; the casing was lowered and latched into the second reentry cone. This time we welded the casing hanger to the reentry cone to prevent it from detaching. We tripped the drilling BHA back into the casing and latched the running tool; the entire assembly with the second reentry cone was lowered through the moonpool at 1830 hr.

On 13 May at 0445 hr, we experienced a VIT camera problem but continued tripping drill pipe while the camera was changed out. The drill pipe was lowered to 4781.77 meters below rig floor (mbrf), the VIT camera was deployed again at 0600 hr, and we picked up the top drive and spaced out in preparation to spud. Hole 1173B was spudded at 0717 hr. We drilled in the 20-in casing with the underreamer and mud motor to 4926.1 mbrf (124.2 mbsf). With the 20-in casing shoe depth at 4922.5 mbrf (120.6 mbsf), we released the casing running tool at 1110 hr; we started tripping out of the hole with the drill pipe and VIT camera. The bit cleared the seafloor at 1225 hr and the rig floor at 2315 hr.

Logging While Drilling

As soon as the tools were laid down, we started assembling the LWD/MWD BHA at 0030 hr on 14 May. The Anadrill engineers loaded the radioactive logging sources at 0515 hr. We then picked up the top drive and tested MWD tools at 300 gpm (60 strokes per minute [spm]) and 800-psi standpipe pressure. By 0600 hr we had assembled and tested the 9.875-in bit, LWD bit sub with float, LWD RAB tool, MWD tool, LWD ISONIC tool, LWD azimuthal neutron and density tool, and the LWD crossover sub. We added five drill collars, a tapered drill collar, and six joints of 5.5-in transition drill pipe, for a total length of 139.88 m. We removed the top drive and calibrated the Anadrill drawworks encoder. At 0700 hr on 14 May, we started tripping the drill string down to the seafloor. Unfortunately, we had to stop at 0930 hr (at 1406.81 mbrf) because of an approaching tropical storm (Cimaron). We tripped out of the hole and secured for transit by 1615 hr on 14 May to avoid the approaching storm.

We continued the transit to evade Tropical Storm Cimaron until 0030 hr on 15 May, when the captain felt it was safe to return to the site. The ship arrived back on site at 1100 hr on 15 May. The total transit was 185 nmi and lasted just over 18 hr.

Once we were back on location, the LWD/MWD BHA was assembled, the radioactive sources were loaded, and the tools were tested. We began lowering the LWD/MWD tools to the seafloor at 1330 hr (15 May). When the drill string reached 3876.06 mbrf, the VIT camera was deployed. However, the

camera signal was lost when it reached 102 mbrf. The camera was retrieved, and we found that the camera cable had been damaged in the upper guide horn. Approximately 110 m of cable was cut off, and the cable was reterminated. While this was being done, the drill string was tripped to 4769.57 mbrf. The repaired VIT camera was deployed at 0330 hr on 16 May. While the camera was being lowered to the seafloor, the drill crew assembled extra drill collar stands in preparation for the next site.

The VIT camera reached the top stabilizer/sensor pad on the LWD tool at 0830 hr but could not be lowered past it. The installed VIT guide sleeve (the same one used for the drilling tools) had an internal diameter of 9.5 in, and the external diameter of the stabilizer pad was 9.875 in. The camera was retrieved, the guide sleeve changed to the casing guide sleeve (internal diameter of 27.5 in), and the camera was redeployed at 0830 hr (16 May). The reentry cone came into view at 1002 hr and was reentered in 1.5 hr. The drill string was lowered into the casing while the VIT was retrieved.

The drill string was spaced out in preparation for drilling and the Anadrill LWD/MWD tools were tested. Drilling/logging operations began at 1500 hr on 16 May at 4922.49 mbrf (120.49 mbsf). The drillers attempted to maintain a 50 m/hr rate of penetration (ROP), as the scientists had requested. The effective ROP was lower than this due to the time required to make pipe connections. The average surface drilling parameters were a WOB of 4–7 kilopounds (klb) at 60 rpm, a torque of 150–175 A, and a flow rate of 327 gpm (67 spm) with a standpipe pressure of 1250 psi.

LWD/MWD operations continued until 1545 hr (17 May) when Hole 1173B reached a total depth of 5539.00 mbrf (737.10 mbsf). The top drive was disconnected from the drill string and racked back in preparation to pull out of the hole. Due to deteriorating hole conditions, however, the top drive had to be reattached to provide rotation and allow circulation. The maximum overpull was 30 klb. The top drive was removed at 5346.6 mbrf. During the trip out of the hole, the LWD tools were recording the entire interval and the speed was controlled at 70 m/hr from 5221.90 to 5171.90 mbrf (420.00–370.00 mbsf) to evaluate LWD ISONIC velocity data quality. The drill bit cleared the seafloor at 2135 hr on 17 May.

Heave Compensation Experiments

Two experiments were conducted during the drilling of the hole to assess the efficacy of the shipboard active heave compensation (AHC) system. We used the MWD tool to measure downhole drilling parameters, including downhole WOB, torque, and bit bounce. These measurements are made using paired strain gauges near the base of the MWD collar, are transmitted to the surface for recording, and are not in downhole memory. Strong MWD pressure signals were recovered at the surface using MWD pulse rates of 3 bits per second (bps) at up to 5500 mbrf depth in Hole 1173B. Surface data from the rig instrumentation system (RIS), including surface rotations per minute, torque, WOB, ship heave, pitch, and roll, were recorded synchronously. Sea states were recorded up to 2 m and heave to 1.5–2 m during drilling at Site 1173.

For the first experiment six intervals were drilled with the AHC off (4955.7–4974.66, 5080–5099.29, 5224.15–5243.31, 5387.65–5406.87, 5464.62–5493.94, and 5527–5531.98 mbrf). During these intervals, drilling proceeded using the passive heave compensation system that has been used for most ODP drilling prior to Leg 189. The second experiment consisted of drilling four intervals with the AHC preloaded, which allows the driller to set the surface weight prior to putting the bit on the bottom of the hole (5329–5358, 5406–5435, 5435–5464, and 5522–5527 mbrf). Whether or not this practice is effective in controlling penetration rates is debatable.

Real-time shipboard observations suggest that the AHC damps high-frequency variations in uphole rotations per minute and torque, as well as the high-frequency variation in downhole WOB. The comparison of downhole MWD parameters with the surface information will be analyzed postcruise to evaluate the shipboard heave compensation system and drilling practices.

Hole 1173C

Logging While Drilling

Hole 1173C was designed to obtain LWD/MWD logs from the uppermost section that was cased off in Hole 1173B. The ship was offset 50 m to the northwest of Hole 1173B, and Hole 1173C was spudded at 2320 hr on 17 May. The LWD/MWD drilling/logging operations were conducted from the seafloor (4801.90 mbrf) to a total depth of 4976.90 mbrf (175.00 mbsf), which was reached at 0500 hr on 18 May. The ROP was controlled at 60 m/hr and the effective ROP (including the time required to make pipe connections, etc.) was 30.9 m/hr. The average surface drilling parameters were a WOB of 4 klb at 60 rpm, a torque of 150 A, and a flow rate of 327 gpm (67 spm) with a standpipe pressure of 1250 psi.

The drill string cleared the seafloor at 0650 hr on 18 May; the LWD/MWD BHA reached the rig floor at 1430 hr. The LWD/MWD tools were disassembled, and the drill bit cleared the rotary table at 1655 hr on 18 May. One of the two seafloor positioning beacons was retrieved, and the other was turned off and left on the seafloor for use later in the leg when we would conduct ACORK operations. The drilling equipment was then secured for the transit to the next site.

Site 808

Hole 808H

After the 1-hr, 8-nmi transit from Site 1173, we arrived at Site 808 at 1800 hr on 18 May. During the transit the drill crew slipped and cut the drill line. The seafloor positioning beacon was deployed at 1937 hr. The precision depth recorder indicated a water depth of 4674.5 mbsl (4685.4 mbrf). The vessel was offset 1 km west (upcurrent) to allow assembly of the casing while the ship drifted with the current. The reentry cone was positioned on the moonpool door. The drill floor was rigged up to run 20-in casing, and the drill crew started running the 20-in casing at 2215 hr on 18 May. The casing string included a shoe joint (10.63 m), 12 joints of casing, and a short (pup) joint of casing attached to the casing hanger. The casing running tool was attached to the casing hanger. A compound (Baker-Loc) was applied to each threaded connection to ensure that it did not come apart, and all casing connections were tack-welded. The casing was lowered and latched into the reentry cone by 0515 hr on 19 May. We then assembled the drilling BHA that included an 18.5-in drill bit, a 22-in underreamer (Smith Service 15000 DTU), a positive-displacement mud motor (Drilex Model D825MSHF), 16 drill collars, and the casing running tool. The drilling BHA was lowered into the reentry cone and casing and latched into the casing hanger. The casing, reentry cone, and drilling BHA were deployed through the moonpool at 0900 hr on 19 May. The drilling BHA (160.14 m) extended 3.54 m beyond the casing assembly (156.60 m).

The casing, reentry cone, and drilling BHA had been lowered to 3606.94 mbrf by 1500 hr on 18 May. The VIT camera was deployed, and we continued lowering the pipe to 4646.12 mbrf, where we spaced out the drill pipe in preparation to spud. Hole 808H was spudded at 1805 hr on 18 May. The casing was drilled into the seafloor from 0 to 126.70 mbsf (4685.00–4811.7 mbrf). While drilling ahead, we circulated sepiolite mud sweeps at 4710, 4735, 4780, 4792, 4802, and 4811 mbrf.

At 0230 hr on 20 May the downhole positive-displacement motor (mud motor) that provides rotational torque to the underreamer and drill bit appeared to stop working. At 0430 hr, we decided to pull the casing and reentry cone back up to the ship and replace the mud motor. The bit cleared the seafloor at 0615 hr on 20 May. The pipe trip continued until 0645 hr, when we began to recover the VIT camera; the pipe trip resumed at 0815 hr. The casing and reentry cone were set on the moonpool doors at 1625 hr. After unlatching the running tool from the casing, the BHA was taken apart until the mud motor was reached.

The mud motor was tested from 1800 to 1830 hr. The mud motor would not rotate when we pumped seawater through it at 165 gpm at 1025 psi. Testing prior to drilling operations showed that it freely rotated at 275 gpm with 125 psi. The mud motor was laid down, and the drill bit cleared the rig floor at 1910 hr on 20 May, ending Hole 808H.

Hole 808I

After its installation at 1915 hr on 20 May, the backup mud motor was successfully tested with circulation rates of 25 spm at 50 psi, 50 spm at 225 psi, and 70 spm at 450 psi. The BHA and casing running tool were attached to it, and the entire assembly was lowered and latched into the casing and reentry cone; it was deployed through the moonpool at 2205 hr.

When the bit was at 3809.22 mbrf, the VIT camera was deployed. We continued tripping down to 4646.12 mbrf, where we spaced out the drill string in preparation to spud. Hole 808I was spudded at 0720 hr; the seafloor depth was 4686 mbrf. We successfully drilled the casing down to 160.14 mbsf (4845.14 mbrf). The average drilling parameters were a WOB of 5–15 klb and a flow rate of 400–550 gpm (80–110 spm) with 900–1150 psi.

The casing running tool was released at 2110 hr on 21 May, and the bit cleared the seafloor at 2245 hr on 21 May. When the drill string had reached 4588.59 mbrf, the VIT camera was retrieved. With the bit at 124.06 mbrf, the casing running tool was removed, the BHA was disassembled, and the mud motor and underreamer were flushed with freshwater.

On 22 May at 1245 hr, the LWD/MWD BHA was made up with a new 9.875-in bit. The MWD mud pulse communications were tested with a flow rate of 305 gpm (61 spm). The trip down to the seafloor started at 1630 hr; the VIT camera was launched at 0030 hr when the bit had reached 4309.02 mbrf. While the VIT camera was being lowered, the drill crew slipped and cut the drill line. The drill string was tripped to 4654.13 mbrf, and we started searching for the reentry cone at 0315 hr on 23 May. The cone was successfully reentered at 0345 hr. The LWD/MWD tools were lowered from mudline (4686 mbrf) to 141.4 mbsf (4827.4 mbrf). After the VIT camera was retrieved at 0630 hr, the drill string was lowered to 160.14 mbsf (4846 mbrf). We began LWD/MWD logging/drilling at 0745 hr on 23 May.

The goal was to log/drill at a controlled rate of 50 m/hr. With connection times, the average ROP from 4846.14 mbrf (160.14 mbsf) to 5214.54 mbrf (528.54 mbsf) was 22.9 m/hr. Sepiolite mud sweeps (15 bbl) were pumped at 329, 413, and 471 mbsf to help remove cuttings and improve hole conditions. The drilling parameters used were a WOB of 5–20 klb, torque of 175–225 A, and a flow rate of 67 spm (327 gpm) with 1250–1350 psi standpipe pressure.

On 24 May, the logging/drilling continued from 5214.54 mbrf (528.54 mbsf) to 5435.72 mbrf (749.72 mbsf), and the average ROP dropped to 21.0 m/hr. Twenty-barrel sepiolite mud sweeps were circulated at 557 and 634 mbsf, with a 30-bbl sweep at 749 mbsf.

Prior to continuing deeper into the hole, a wiper trip was made to determine hole conditions from 5435.72 mbrf (749.72 mbsf) to the casing shoe at 4846.14 mbrf (160.14 mbsf). The drill string was pulled with the top drive to 5230.73 mbrf (544.73 mbsf) with a maximum overpull of 20 klb and torque of 400 A. The top drive was then removed and the string pulled to 4827.4 mbrf (141.4 mbsf). The drill string was tripped back to 5256.51 mbrf (570.51 mbsf), where we picked up the top drive and reamed down to 5435.72 mbrf (749.72 mbsf). One tight spot was encountered at 5413 mbrf (727 mbsf).

Logging/drilling then continued from 5435.72 mbrf (749.72 mbsf) to 5474.26 mbrf (788.26 mbsf). The average ROP dropped to 15.7 m/hr as a result of the wiper trip and the time needed to make pipe connections. One 30-bbl sepiolite mud sweep was circulated at 759 mbsf. The drilling parameters were a WOB of 15–20 klb at 60 rpm, torque of 200–300 A, and a flow rate of 67 spm (327 gpm) with 1500 psi standpipe pressure.

On 25 May, LWD/MWD logging/drilling continued from 5474.26 mbrf (788.26 mbsf) to 5676.26 mbrf (990.26 mbsf). Sepiolite mud sweeps (20 bbl) were circulated at 846, 923, and 968 mbsf.

The décollement was encountered at 5654 mbrf (968 mbsf). We experienced drilling problems (high torque and high pump pressures) from 1115 to 2245 hr. Efforts to improve hole conditions included circulation, mud sweeps, and reaming up and down with the drill string. A short wiper trip was made from 5676.26 mbrf (990.26 mbsf) to 5615.39 mbrf (929.39 mbsf). During the wiper trip, the maximum overpull was 25 klb, maximum torque was 550 A, and the maximum pump pressure was 2200 psi.

Logging/drilling operations continued from 5676.26 mbrf (990.26 mbsf) to 5695.51 mbrf (1009.51 mbsf). The average ROP dropped to 13.3 m/hr due to connection times, hole conditioning, and the wiper trip. The LWD/MWD logging/drilling parameters were a WOB of 15–20 klb at 60 rpm, torque of 275–350 A, and a flow rate of 67 spm (327 gpm) with 1550 psi standpipe pressure. Sepiolite mud sweeps (20 bbl) were pumped at 958, 961, and 990 mbsf. Another wiper trip was made from 5695.51 mbrf (1009.51 mbsf) to 5615.39 mbrf (929.39 mbsf).

Most of 26 May was spent fighting the poor hole conditions, making wiper trips, and troubleshooting an overheating top drive. LWD/MWD logging/drilling extended from 5695.51 mbrf (1009.51 mbsf) to 5743.55 mbrf (1057.55 mbsf). The LWD/MWD logging/drilling parameters were a WOB of 15–20 klb at 60 rpm, and torque of 275–350 A with a maximum of 600 A. The pump pressure was 60 spm (300 gpm) with 1550 psi standpipe pressure. At 2330 hr, the drill string became stuck with the bit at 5702.08 mbrf (1016.08 mbsf). We were unable to rotate the drill string or move it up or down. Rotation and movement were successfully regained at 0045 hr on 27 May. We decided not to continue operations in this hole and began to trip out using the top drive for rotation and circulation up to 5432.72 mbrf (746.72 mbsf). The top drive was removed, and the bit cleared the seafloor at 0615 hr. The drill collars were racked back in the derrick and the LWD/MWD logging tools were laid down. The drill bit cleared the rig floor at 1710 hr on 27 May, ending Hole 808I. The thrusters and hydrophones were raised, and the seafloor positioning beacon was turned off. We began the transit to Kochi at 1715 hr on 27 May.

Heave Compensation Experiments

At Site 808, we used the MWD tool to measure downhole drilling parameters, including downhole WOB, torque, and bit bounce. Given the strong MWD pressure signals obtained at the surface during Site 1173 MWD operations, we increased the MWD data transmission rates at Site 808 to 6 bps.

Surface data from the RIS, including surface rotations per minute, torque, WOB, ship heave, pitch, and roll, were recorded synchronously. Ship heave was between 0.5 and 1.5 m during drilling at this site.

Eight experiments were conducted while drilling ahead with the AHC off (4917.15–4946.04, 5013.15–5032.10, 5118.59–5137.87, 5214.54–5233.73, 5320.17–5349.09, 5416.50–5435.72, 5522.33–5541.59, and 5724.37–5733.96 mbrf). One of these intervals (5522.33–5541.49 mbrf) was partially drilled with the AHC preloaded at a set surface weight to evaluate this practice in comparison to similar tests conducted at Site 1173. The comparison of downhole MWD parameters with the surface information will be analyzed postcruise to evaluate the shipboard heave compensation system and to compare drilling conditions with those encountered at Site 1173.

Transit from Hole 808I to Kochi, Japan, and Kochi Port Call

The 96-nmi transit to Kochi, Japan, began at 1718 hr on 27 May and ended at 1118 hr on 28 May. Since the local port authorities would not allow the vessel into the harbor before 1130 hr, the harbor pilot was aboard at 1126 hr, and the first line ashore was at 1230 hr. After customs and immigration formalities were completed at 1345 hr, 20 scientific staff members departed and nine boarded the ship. The afternoon was filled with public tours for local television stations, newspapers, government officials, Kochi University officials, and university students. Nearly 100 people toured the ship.

At 1345 hr, we began offloading the LWD/MWD tools, 10 joints of 20-in casing, 30 joints of 10.75-in casing, a broken mud motor, a 22-in underreamer, a broken air conditioner compressor, and three-dimensional seismic computer work stations. Equipment loaded included food, scientific equipment for the ACORK and thermistor experiments, 64 joints of 4.5-in casing, nine external casing packers, 11 joints of 10.75-in screened casing, two ROV platforms, one replacement mud motor (Drilex 7.75 in), inner core barrels, ten 0.75-in casing centralizers, four 0.5-in casing centralizers, one 30-ft knobby drill pipe, one 20-ft knobby drill pipe, one tapered drill collar, one pup joint of 16-in casing, one 16-in casing hanger, and a few steel I-beams. Loading/offloading operations were completed at 0330 hr on 29 May, and the equipment and casing were stored and secured for departure.

Return to Site 1173 for ACORK installation

Following Site 808 LWD/MWD operations and the short port call in Kochi, we returned to Hole 1173B. The Kochi harbor pilot boarded the ship at 0742 hr, and the last line away was at 0800 hr on 29 May. After the pilot departed, we began the transit back to Site 1173 at 0812 hr. After traveling 104 nmi in 9.3 hr, we arrived at Hole 1173B at 1730 hr on 29 May, started lowering the thrusters, and turned the seafloor positioning beacon on.

Our first objective was to reenter Hole 1173B and open the 9.875-in LWD hole up to 17.5 in before installing the ACORK. We began by making up the BHA, which included a 9.875-in bit sub with float valve, a 17.5-in hole opener, crossover subs, and drill collars. At 1910 hr, the ship was in position over Hole 1173B. The bit was lowered to 3534.3 mbrf, where the VIT camera was deployed at 0345 hr on 30 May. The bit was lowered to 4794 mbrf, and we began to search for the reentry cone at 0645 hr. Hole 1173B was reentered at 0832 hr. While retrieving the VIT camera, the drill string was lowered into the casing to 4926 mbrf (123.49 mbsf).

We then drilled with the hole opener to a total depth of 5537 mbrf (735.10 mbsf). The AHC was turned off because of ship heaves of 2.8–3.3 m while we drilled the interval from 5133 to 5181 mbrf.

Twenty-barrel sepiolite mud sweeps were pumped to maintain good hole conditions at 177, 235, 292, 350, 388, 446, 504, 552, 590, 648, and 735 mbsf. The drill string was worked through tight spots at 379–389 and 542–552 mbsf. The average drilling parameters were a WOB of 5–10 klb, top drive rotation of 60 rpm, top drive torque of 200–400 A (maximum of 600 A), and pump pressures of 1350–1800 psi at 120–140 spm.

Before pulling out of the hole, we circulated two 60-bbl sepiolite mud sweeps while the bit was at 735.1 mbsf. The trip out of the hole started at 0800 hr on 1 June. Tight spots at 670, 650, 590, and 495.1 mbsf required rotation and circulation. After the bit cleared the seafloor at 1420 hr on 1 June, from 1515 to 1645 hr the drill line was slipped and cut. The bit reached the rig floor at 0230 hr on 2 June, the drill collars were racked back in the derrick, and the bit and hole opener were laid out.

While opening the hole, the moonpool area was prepared for assembling ACORK screens, packers, and casing. A working surface across the moonpool doors was created with I-beams and floor gratings. Tools and supplies were staged in the moonpool area, including the 10.75-in casing centralizers, steel banding, tie wraps, and so forth. The pneumatic umbilical cable reel was set forward of the moonpool area by the drill collar racks; jack stands were welded to I-beams to support the umbilical reel.

The ship was offset ~5 nmi west of Hole 1173B in preparation for assembling the ACORK screens, packers, and 10.75-in casing. From 0230 hr on 2 June to 1730 hr on 3 June, we assembled 54 joints of 10.75-in casing, five screen joints, and four external casing packers. The total length of the ACORK from the casing shoe to the landing joint was 727.77 m, and the weight was ~90,000 lb. During this operation, the umbilical cable, casing centralizers, and strapping (tie-wraps and banding material) were attached to the casing in the moonpool. A 0.25-in outer-diameter stainless steel tube was joined between the lowermost screen and packer. Above this the umbilical was hydraulically connected to the bottom and top of each of the screens and packers.

The casing handling equipment was removed from the rig floor by 1800 hr on 4 June. We then moved the ACORK head, ported sub assembly, and 10.75-in casing landing joint from the main deck to the drill floor. After this was attached to the ACORK casing string, the complete assembly was lowered to and hung off the moonpool doors. The casing running tool was released at 2055 hr on 3 June, and we started assembling the drilling BHA. The BHA included a 9.875-in pilot bit, bit sub with float valve, 17-in underreamer, crossover sub, mud motor, crossover sub, six 8.25-in drill collars, crossover sub, 23 stands of 5.5-in drill pipe, one short (5 ft) joint of drill pipe, crossover sub, ACORK stinger, motor-driven core barrel latch sub, and the casing running tool. The total length of the drilling BHA was 737.83 m. Assembly of the drilling BHA was completed at 0500 hr on 4 June.

Once the drilling BHA and ACORK assembly was completed, the final connections of the umbilical to the ACORK head were made. Lowering the ACORK assembly into water in the moonpool purged the air from the stainless steel tubing. From 0800 to 0900 hr on 4 June, the complete assembly was lowered to 1143.3 mbrf. We then deployed the VIT camera to confirm the spacing of the drill bit/underreamer in relation to the bottom of the casing and to verify the proper functioning of the underreamer and mud motor. Once the VIT camera was recovered, the drill string was lowered to 2144.49 mbrf in preparation for the transit back to Hole 1173B. Two 30-ft joints and one 20-ft joint of knobby drill pipe were included at the top of the drill string to provide additional strength to withstand the stress while returning to the site. The transit in dynamic positioning (DP) mode began at 1430 hr on 4 June.

We had begun assembling the ACORK ~5 nmi west of Hole 1173B at 0230 hr on 2 June. Because of the current, we had to allow the ship to drift while we made up the casing. By the time we had

finished assembling the ACORK and had lowered it to 2144 mbrf, the ship had drifted 26 nmi east of Hole 1173B at 1430 hr on 4 June. During the transit back to Hole 1173B, we averaged 0.5 nmi/hr and were back on location at 0035 hr on 7 June.

When the drill string had been lowered to 3708.41 mbrf, the VIT camera was deployed. Once the drill string was at 4790.03 mbrf (0630 hr on 7 June), we began the search for Hole 1173B. At 0840 hr, we reentered Hole 1173B and lowered the drill string to the bottom of the casing. We attached the top drive and began to drill in the ACORK. We continued to observe the operations with the VIT camera until it stopped working at 1320 hr (7 June). After 35.5 hr of drilling, the ACORK was landed, and we reached the total depth of 732.71 mbsf at 1855 hr on 8 June. The lowermost 86 m drilled very slowly, taking ~19 hr to penetrate. The drilling parameters increased with depth, with drag increasing to 20–40 klb, and pump strokes per minute increasing from 70 to 130 spm as the standpipe pressure increased from 700 to 2800 psi. The WOB was 15–20 klb.

At 1900 hr on 9 June, the go-devil shifting tool was deployed to divert the flow path so we could inflate the packers. An increase in pressure at 2030 hr indicated that the ported sub assembly had been shifted. By 2200 hr, the packers had been inflated and the spool valves shifted.

Our next step was to release the casing running tool so that the drilling BHA could be removed, leaving the ACORK assembly installed. At 2030 hr on 9 June, we attempted to release the casing running tool, but, unfortunately, it would not release. At 2200 hr, the VIT camera was deployed to observe the running tool. We maneuvered the ship in a 40-m circle as the drill string was worked up and down with torque to release the running tool. After 7.5 hr, the running tool finally released, and the drilling BHA was raised one joint to confirm this.

After the VIT camera was retrieved by 0715 hr on 9 June, we began assembling the ROV platform on the moonpool doors. The deployment bridle and dual acoustic release mechanism were connected to the logging wireline; the entire assembly was lowered into the moonpool at 0915 hr on 9 June. The ROV platform had landed on the ACORK and was released at 1355 hr.

Once the logging wireline had been retrieved, we began tripping the drilling BHA back up to the rig floor. The bit cleared the seafloor and ACORK head at 2125 hr. When the bit was at 908 mbrf (0445 hr on 10 June), a 5-ft drill pipe joint failed at a pin connection, and the entire drilling BHA was lost. This occurred when the failed pin connection was in the lower guide horn one joint below the rig floor. The following equipment was lost: a 9.875-in bit, six crossover subs, a 17-in underreamer, a mud motor, eight 8.25-in drill collars, 81 joints of 5.5-in drill pipe, one 5.5-in drill pipe pup joint, an ACORK stinger sub, a motor-driven core barrel (MDCB) latch sub, the casing/ACORK running tool, one tapered drill collar, and nine joints of 5-in drill pipe.

The next operational step was to drill out below the end of the 10.875-in casing to allow fluid/pressure communication between basement and the deepest ACORK monitoring zone. We decided to use the RCB coring system. Eight drill collars had to be picked up from the drill collar rack, measured, and made up to replace those we had just lost. The top sub and head sub were added, and the RCB core barrel space out was checked. The remaining drill collars that were racked in the derrick were added to the RCB BHA. We started lowering the bit to the seafloor at 0545 hr on 10 June. When the bit was at 3280 mbrf, tripping of the pipe was stopped to allow the drill line to be slipped and cut. We also used this time to replenish the drill pipe available in the racker. Twenty-one joints of 5.5-in drill pipe were taken from the riser hold, made into stands, and placed in the pipe racker.

At 1900 hr on 10 June, the upper guide horn (UGH) was removed, the VIT camera was deployed, and the UGH was reinstalled. At 1945 hr we resumed lowering the drill string to 4780.03 mbrf, where

it was spaced out for reentry. The search for the reentry cone began at 2230 hr. The 30-in-diameter ACORK head was reentered at 2328 hr.

Problems arose at 2330 hr when the RCB coring BHA encountered a tight spot in the casing at 4608 mbrf (4.14 mbsf). The BHA finally passed through the tight spot at 0145 hr on 11 June. The trip continued to 5327 mbrf (575 mbsf), where we began to retrieve the VIT camera; it was back on board at 0515 hr.

The trip continued to 5500 mbrf (699.00 mbsf), where the top drive was picked up. The hole was washed and reamed to 5539 mbrf (737.1 mbsf). The drill string was spaced out, and RCB coring began. Drilling Core 196-1173B-1R lasted from 0900 to 1300 hr and cored the interval from 5539 mbrf (737.1 mbsf) to 5548 mbrf (746.8 mbsf). A problem was identified with the coring wireline and the oil saver sub that required a slip and cut of the wireline. This delayed the retrieval of Core 196-1173B-1R until 1545 hr on 11 June.

Core 196-1173B-2R took 7.25 hr to cut from 5548.7 mbrf (746.8 mbsf) to 5553.60 mbrf (751.7 mbsf). Slow penetration rates and increased pump pressure suggestive of core jamming led us to pull this core before it had penetrated the full length. The core was on deck at 0030 hr on 12 June. Core 196-1173B-3R was taken from 5553.6 mbrf (751.70 mbsf) to 5558.5 mbrf (756.60 mbsf). Coring operations were stopped at 756 mbsf on 12 June at 0500 hr, as the time allotted for coring had expired. Hole 1173B reached a total depth of 5558 mbrf (756 mbsf). The top drive was used to pull out from 5558.5 mbrf (756 mbsf) to 5500 mbrf (699 mbsf); the top drive was then racked back, and the trip out of the hole continued. The bit cleared the seafloor at 0745 hr and the rig floor at 1615 hr on 12 June.

The final step in completing the Hole 1173B ACORK was to set a bridge plug at 722 mbsf inside the 10.75-in casing. The bridge plug (Weatherford model 53PBP.1001; 10.75-in, 40.5-lb mechanical set cast-iron bridge plug) and 10.75-in mechanical setting tool (model 53MST.1002 with a crossover to 4.5-in American Petroleum Institute regular threads) were assembled to two drill collars, one tapered drill collar, and six joints of 5.5-in drill pipe. This bridge plug BHA was lowered to 3275 mbrf, where the VIT camera was deployed. The drill pipe was lowered to 4778 mbrf, where the top drive was picked up for drill string space out and reentry. The search for the reentry cone began at 0415 hr on 13 June. The 30-in-diameter ACORK head was reentered at 0610 hr.

The bridge plug was run in the hole to 5268 mbrf (466.3 mbsf). The VIT was retrieved at 0900 hr. The trip continued to 5498 mbrf (696 mbsf). The top drive was picked up and the drill string spaced out to set the bridge plug at 722 mbsf. The bridge plug requires 10 revolutions of right-hand rotation to set the upper slips. When right-hand rotation was applied to the drill string, the torque built to ~600 A in only eight revolutions. Numerous unsuccessful attempts were made from 1030 to 1200 hr to achieve the required 10 revolutions. While holding torque in the string, the crew worked the string up and down 15 m with no drag or overpull.

We then started pulling the pipe up the hole while trying to set the bridge plug at every stand; it was a wet trip. When the bridge plug reached 466.3 mbsf and the connection was made, the drill pipe at the rig floor had no water in it. Immediately upon pulling up on the next stand, overpull was observed, and then the sequence of actions to set the packer was initiated. Forty thousand pounds of overpull was held for 5 min to set the packer. Then 5 klb of weight was set down on the packer. A second overpull of 40 klb was applied and then bled off to neutral weight. The drill string was rotated to the right to release the running tool from the bridge plug. The torque climbed to 250 A with three rotations and then fell to 150 A, indicating that the bridge plug was set.

The drill string was then raised to 437 mbsf. After removing the top drive, tripping operations continued. The driller observed that the drill string weight appeared to be ~30 klb too low. The trip continued until the bottom of the pipe should have been at 470.95 mbrf when a failed 5-ft drill pipe joint cleared the rotary table at 2400 hr. Five joints of 5-in drill pipe were removed from service: four had been bent and one had parted in the tube body. The following equipment was lost: bridge plug running tool, bit sub, two 8.25-in drill collars, one tapered drill collar, six joints of 5.5-in drill pipe, three crossover subs, and 40 joints of 5-in drill pipe. The forty-first joint of drill pipe above the BHA parted due to compression bending ~8.4 m from the tool joint shoulder. Analysis of the drilling data suggests that the bridge plug had set at 466 mbsf. The 471-m length of lost equipment suggests that the parted drill pipe is at the top of the ACORK head assembly. Since the bridge plug had set, we determined there was nothing more that could be done at Hole 1173B and began the transit to Hole 808I at 0000 hr on 14 June. We were unable to recover the seafloor positioning beacon once it reached the surface.

Hole 808I ACORK Operations

After finishing ACORK operations in Hole 1173B, we returned to Hole 808I. Despite the short distance between Sites 1173 and 808, we were unable to transit in DP mode while tripping the pipe because of the current. We arrived back at Hole 808I at 0140 hr on 14 June after a 1.5-hr transit. The seafloor positioning beacon was turned on at 0240 hr. Because of our drill pipe loss at the end of Hole 1173B, our operations began with retrieving 75 additional joints of 5-in drill pipe from the riser hold, making them up into stands, and putting them in the drill pipe racker.

During LWD/MWD drilling earlier in the leg, Hole 808I had been drilled with a 9.875-in bit to 5743 mbrf (1057 mbsf). Our next step in preparing this hole for an ACORK was to open the existing 9.875-in hole to 17.5 in. A drilling BHA was assembled with a 9.875-in pilot bit and a 17.5-in hole opener. The aluminum pipe protectors were removed from six joints of 5.5-in drill pipe so these joints could be used as transition joints in the BHA. Once this was assembled, the bit was lowered to 4380 mbrf, and the VIT camera was deployed at 2115 hr on 14 June; the drill line was slipped and cut while the camera was being lowered. At 2315 hr we resumed lowering the drill string until it reached 4669 mbrf, where it was spaced out for reentry.

We began the search for the reentry cone at 0000 hr on 15 June. Hole 808I was reentered at 0210 hr. Once we were in the hole, the drill pipe was lowered to 4812 mbrf (126 mbsf), and the top drive was picked up at 0345 hr. The VIT camera was retrieved; at 0615 hr we started drilling ahead at 4846 mbrf (160 mbsf). Twenty-barrel mud (sepiolite) sweeps were pumped every 40–50 m. The hole opening continued until we reached a total depth of 975.3 mbsf at 2025 hr on 17 June. We circulated a 40-bbl mud sweep and then started pulling out of the hole. The bit cleared the seafloor at 0730 hr on 18 June.

After the drilling tools were secured, we began moving the ship ~70 nmi upcurrent (west-northwest; ~250°) to begin assembling the ACORK. The transit began at 1600 hr on 18 June. During the transit, the drill floor crew prepared to run the 10.75-in ACORK casing. As soon as the transit ended at 0000 hr on 19 June, we began assembling the ACORK.

The first screen joint was moved to the rig floor; a casing collar was welded to the bottom pin connection to act as a guide shoe. The lowermost packer was made up as the second joint in the string, and a single 0.25-in stainless steel tube was run from the top of the screen to the bottom of the packer. The hydraulic umbilical was started at the top of the lowermost packer. As the casing,

screens, and uppermost packer were assembled, hydraulic connections were made at the top and bottom of each screen and packer. Three centralizers were added to each joint, and the umbilical was strapped to the casing near each centralizer with 0.625-in metal banding.

During the remainder of 19 June, 68 additional joints of 10.75-in casing and five more screen joints were added to the ACORK assembly. From 0000 to 0500 hr on 20 June, eight more casing joints, one packer, and the landing joint were added to the string. At 0500 hr the casing running tool, ACORK head, and ported sub assembly were moved to the rig floor and attached to the top of the landing joint. The total length of the ACORK assembly was 964.32 m. The completed ACORK assembly was lowered below the rig floor and hung off the moonpool doors by 0700 hr on 20 June.

The next step was to assemble the drilling BHA that would pass through the ACORK assembly, allowing the bit and underreamer to extend below the guide shoe on the bottom of the ACORK. First, we had to remove the crossover subs that came with the mud motor, as they had 7.625-in instead of 6.625-in connections; an ODP crossover sub connected the mud motor to the 8.25-in drill collar above. We then discovered that the crossovers for the underreamer were incorrectly listed in inventory as 4.5-in regular connections and therefore could not be securely made up to those on the underreamer. Because of the previous BHA losses on this leg, no other appropriate crossovers were available, so we welded one of the existing crossover subs directly to the underreamer. The other crossover required the fabrication of a spacer ring to fill a gap between the mating shoulders before it could be welded to the underreamer. A total of 9 hr was required for these modifications.

The remainder of the drilling BHA was assembled without additional problems. The complete drilling BHA contained the following components: 9.875-in bit, bit sub with float valve, three crossover subs, 17-in underreamer, crossover sub, mud motor, crossover sub, nine 8.25-in drill collars, crossover sub, 91 joints of 5.5-in drill pipe, one 5-ft 5.5-in drill pipe pup joint, crossover sub, landing saver sub, one 8.25-in drill collar pup joint, jet sub, MDCB latch sleeve sub, the casing running tool, two 8.25-in drill collars, one tapered drill collar, six joints 5.5-in drill pipe, and crossover sub. The total length of BHA from the running tool to the bit was 975.43 m.

When the drilling BHA was assembled and the casing running tool latched to the ACORK head, the complete assembly was lowered so that the final umbilical connections could be made in the moonpool area. After the ACORK assembly was dipped into the water for purging air from the hydraulic lines, the ACORK assembly and drilling BHA were lowered until the bit was at 1294 mbrf. At 0400 hr the VIT camera was deployed so that we could verify the space out of the underreamer with respect to the bottom of the casing as well as the functioning of the mud motor and underreamer. Once these tests were finished, the VIT camera was recovered at 0545 hr on 21 June. We then lowered the pipe to 3462.15 mbrf, where it was kept during the transit back to the site in DP positioning mode.

During the entire assembly/testing of the ACORK and the drilling BHA, the ship was in a controlled drift back toward Hole 808I. The initial offset from the site was ~70 nmi at 0000 hr on 19 June. We arrived back at Hole 808I at 0330 hr on 22 June.

On 21 June (0620–0645 hr), the *Aso Maru* arrived to deliver two engineers to assist with the thermistor string deployment later in the leg. A number of small packages, fresh fruit, and vegetables were also delivered. Two small pieces of failed drill pipe were offloaded for forensic analysis. Also, during the DP transit back to the site, 113 aluminum pipe protectors were removed from the drill pipe, as they would not be used.

We resumed lowering the drill pipe once we were back on site and ran the pipe down to 3798 mbrf, where we stopped to deploy the VIT camera at 0430 hr on 22 June. The pipe trip then

continued at 0500 hr. Once the drill string reached 4662 mbrf, it was spaced out in preparation for reentering Hole 808I. After only 20 min, Hole 808I was reentered at 0805 hr on 22 June.

The drill bit/mud motor and casing shoe encountered some resistance passing through the reentry cone hanger at 4686 mbrf. After lowering the drill string to 4842 mbrf (156 mbsf), we began washing and drilling in the ACORK, reaching 5269 mbrf (583 mbsf) at 2400 hr on 22 June. Twenty-barrel mud (sepiolite) sweeps were circulated at 295, 430, 497, 555, and 574 mbsf. The drilling parameters were a WOB of 0–20 klb with a circulation rate of 100–120 spm and a pressure of 1450–2200 psi.

On 23 June, we continued drilling in the ACORK from 5269 mbrf (583 mbsf) to 5452 mbrf (766 mbsf). The VIT camera had to be retrieved at 2030 hr. Twenty-barrel mud (sepiolite) sweeps were circulated at 660, 670, 747, and 764 mbsf. The penetration rate for 22 June was 7.6 m/hr. The drilling parameters were a WOB of 10–20 klb and a circulation of 120 spm with a pressure of 2200 psi.

From 24 to 26 June, the ACORK was advanced from 5452 mbrf (766 mbsf) to 5611 mbrf (925 mbsf) with a penetration rate of only ~2 m/hr. Twenty-barrel mud (sepiolite) sweeps were circulated every 10–20 m. The drilling parameters were a WOB ranging up to ~180 klb and a circulation of 70–120 spm with a pressure up to 2200 psi.

As the penetration rate was so low and any increase in WOB would cause concern for the safety of the casing and drill string, we decided to deploy the VIT camera at 1400 hr on 26 June and perform some WOB tests. Once the camera was on the bottom at 1615 hr, we noted that the drill string, ACORK head, casing, and reentry cone all appeared to be intact. We then attempted to increase the WOB to the maximum deemed safe and saw no significant increase in penetration or bending of the drill string or ACORK. We also tried to raise the drill string to see if recovering the entire assembly was an option; it could not be raised. During these tests, circulation was observed coming out of the reentry cone, which indicated that, although a flow path existed, the casing was being held by skin friction. The VIT was retrieved at 1950 hr on 26 June.

Because it was clear that we could not pull out of the hole, we continued to try to advance the ACORK in the hope that we could advance enough to either latch it in the reentry cone or get it low enough so that it could remain upright on its own. On 27 June, we advanced from 5611 mbrf (925 mbsf) to 5620 mbrf (934 mbsf) or ~0.4 m/hr. Two 100-bbl mud sweeps were pumped at 927 and 929 mbsf, as were two 20-bbl sweeps at 931 and 933 mbsf. The drilling parameters were a WOB of 180 klb and a pump rate of 70–120 spm with a pressure of 1000–2200 psi

From 0000 to 0430 hr on 28 June, we continued to work the drill string, but it would not advance below 5620 mbrf (934 mbsf). In a last-ditch effort, we pumped 500-bbl of heavy (11.3 lb/gal) mud into the hole at 0430 hr and continued to work the pipe until 0730 hr with no success. At this point, we decided to inflate the packers. The circulation sub was shifted open with the wireline-shifting tool. The go-devil was dropped; once it landed, a slow pump rate was used to inflate the two packers and close the spool valves. This was completed at 0900 hr.

We then released the casing running tool at 1100 hr and raised the drill string from 5620 mbrf (934 mbsf) to 5574 mbrf (888 mbsf). Because it seemed unlikely that conditions would allow a bridge plug to be installed, the science party requested heavy mud be placed in the hole, so 100 bbl (10.5 lb/gal) of mud was pumped into the hole. Tripping operations resumed at 1215 hr, with the top drive being racked back and the 20-ft knobby laid out.

The VIT camera was deployed and run in the hole from 1245 to 1315 hr on 28 June to observe the withdrawal of the drilling BHA from the ACORK head. At 1533 hr the drilling BHA came out of the reentry cone, and the ACORK head slowly bent toward the seafloor and went out of sight. The drill string and VIT camera were lowered for a closer inspection, and the ACORK casing was observed to

be bent over the edge of the reentry cone. With the camera, we followed the casing away from the reentry cone. The compass on the camera indicated the casing fell to the north. No damage was seen to the ACORK umbilical, casing, or head. The ACORK head was lying flat on the seafloor, and ~60% of the ACORK head appeared above the seafloor. Most importantly, the underwater mateable connector was sticking straight up so that a submarine or ROV can still connect to download the data.

We started to recover the VIT camera at 1645 hr on 28 June. The drill string was pulled to 4491 mbrf, and knobbies were installed so that the drill string could be hung off during the DP transit back to Hole 1173B. The seafloor positioning beacon was released at 1815 hr. Once the VIT camera was back on board at 1845 hr, the hydrophones were raised, and the ship began the DP transit back to Hole 1173B.

Return to Hole 1173B ACORK

After finishing operations at Site 808, we returned to Hole 1173B to conduct a camera survey of the ACORK. After a 9.25-hr DP transit, the ship arrived at Hole 1173B at 0420 hr on 29 June. The drill string was lowered to 4795 mbrf, and the seafloor search for the reentry cone and ACORK began at 0600 hr. The reentry cone was located at 0618 hr and was observed until 0630 hr. The parted end of the drill pipe was inside the ACORK minicone and did not appear to stick out above it. Other than the fact that the inner bore of the ACORK is unusable, the Hole 1173B ACORK installation appeared to be intact. We began recovering the drill string and the VIT camera at 0630 hr on 29 June. The VIT was retrieved at 1200 hr. When the bit cleared the rig floor (2215 hr), we observed that the underreamer arms had broken off. This may have been one of the problems contributing to our inability to penetrate to the total depth. The transit to Yokohama began at 2215 hr. Leg 196 ended with the first line ashore at 0830 hr on 1 July 2001 in Yokohama.

REFERENCES

Ando, M., 1975. Source mechanisms and tectonic significance of historical earthquakes along the Nankai Trough, Japan. *Tectonophysics,* 27:119–140.

Bray, C.J., and Karig, D.E., 1985. Porosity of sediments in accretionary prisms and some implications for dewatering processes. *J. Geophys. Res.*, 90:768–778.

Carson, B., Suess, E., and Strasser, J.C., 1990. Fluid flow and mass flux determinations at vent sites on the Cascadia margin accretionary prism. *J. Geophys. Res.*, 95:8891–8889.

Fisher, A.T., 1998. Permeability within basaltic oceanic crust. *Rev. Geophys.* 36:143–182.

Fisher, D.M., 1996. Fabrics and veins in the forearc: a record of cyclic fluid flow at depths of <15 km. *In* Bebout, G.E., Scholl, D.W., Kirby, S.H., and Platt, J.P., *Subduction Top to Bottom*. Am. Geophys. Union, Geophys. Monogr., 96:75–89.

Henry, P., Lallemant, S.J., LePichon, X., and Lallemand, S.E., 1989. Fluid venting along Japanese trenches; tectonic context and thermal modeling. *Tectonophysics,* 160:277–292.

Hill, I.A., Taira, A., Firth, J.V., et al., 1993. *Proc. ODP, Sci. Results,* 131: College Station, TX (Ocean Drilling Program).

Isaacs, C.M., Pisciotto, K.A., and Garrison, R.E., 1983. Facies and diagenesis of the Miocene Monterey Formation, California: a summary. *In* Iijima, A., Hein, J.R., and Siever, R. (Eds.), *Siliceous Deposits in the Pacific Region:* Amsterdam (Elsevier), Devl. in Sedimentol. Ser., 36:247–282.

Kanamori, H., 1986. Rupture process of subduction-zone earthquakes. *Annu. Rev. Earth Planet. Sci.,* 14:293–322.

Kastner, M., Elderfield, H., Jenkins, W.J., Gieskes, J.M., and Gamo, T., 1993. Geochemical and isotopic evidence for fluid flow in the western Naikai subduction zone, Japan. *In* Hill, I.A., Taira, A., Firth, J.V., et al., *Proc. ODP, Sci. Results,* 131: College Station, TX (Ocean Drilling Program), 397–413.

Kastner, M., Elderfield, H., and Martin, J.B., 1991. Fluids in convergent margins: what do we know about their composition, origin, role in diagenesis and importance for oceanic chemical fluxes? *Philos. Trans. of the R. S. London A,* 335:243–259.

Kodaira, S., Takahashi, N., Park, J., Mochizuki, K., Shinohara, M., and Kimura, S., 2000. Western Nankai Trough seismogenic zone: results from a wide-angle ocean bottom seismic survey. *J. Geophys. Res.,* 105:5887–5905.

Lallemant, S., Byrne, T., Maltman, A.J., Karig, D.E., and Henry, P., 1993. Stress tensors at the toe of the Nankai accretonary prism: an application of inverse methods to slickenlined faults. *In* Hill, I.A., Taira, A., Firth, J.V., et al., *Proc. ODP Sci. Results,* 131: College Station, TX (Ocean Drilling Program), 103–122.

Mazzotti, S., LePichon, X., Henry, P., and Miyazaki, S., 2000. Full interseismic locking of the Nankai and Japan-West Kuril subduction zones: an analysis of uniform elastic strain accumulation in Japan constrained by permanent GPS. *J. Geophys. Res.,* 105:13159–13177.

Moore, G.F., Taira, A., Bangs, N.L., Kuramoto, S., Shipley, T.H., Alex, C.M., Gulick, S.S., Hills, D.J., Ike, T., Ito, S., Leslie, S.C., McCutcheon, A.J., Mochizuki, K., Morita, S., Nakamura, Y., Park, J.-O., Taylor, B.L., Yagi, H., and Zhao, Z., 2001. Data report: Structural setting of the Leg 190 Muroto Transect. *In* Moore, G.F., Taira, A., Klaus, A., et al., *Proc. ODP, Init. Repts.,* 190 [CD-ROM]. Available from: Ocean Drilling Program, Texas A&M University, College Station TX 77845-9547, USA.

Moore, G.F., Taira, A., Klaus, A., et al., 2001. *Proc. ODP, Init. Repts.,* 190 [CD-ROM]. Available from: Ocean Drilling Program, Texas A&M University, College Station TX 77845-9547, USA.

Moore, J.C., and Vrolijk, P., 1992. Fluids in accretionary prisms. *Rev. Geophys.,* 30:113–135.

Moores, E.M., and Twiss, R.J., 1995. *Tectonics:* New York (W.H. Freeman and Company).

Morgan, J.K., and Karig, D.E., 1995. Kinematics and a balanced and restored cross-section across the toe of the eastern Nankai accretionary prism. *J. Struct. Geol.,* 17:31–45.

Okino, K., Ohara, Y., Kasuga, S., and Kato, Y., 1999. The Philippine Sea: new survey results reveal the structure and history of marginal basins. *Geophys. Res. Lett.,* 26:2287–2290.

Park, J.-O., Tsuru, T., Kodaira, S., Nakanishi, A., Miura, S., Kaneda, Y., and Kono, Y., 2000. Out-of-sequence thrust faults developed in the coseismic slip zone of the 1946 Nankai earthquake (Mw = 8.2) off Shikoku, southwest Japan. *Geophys. Res. Lett.,* 27:1033–1036.

Plank, T., Stern, R., and Morris, J., 1998. The subduction factory science plan, MARGINS Program. *Nat. Sci. Found.* <http://www.soest.hawaii.edu/margins/SubFac.html>

Seno, T., 1977. The instantaneous rotation vector of the Philippine Sea plate relative to the Eurasian plate. *Tectonophysics,* 42:209–226.

Seno, T., Stein, S., and Gripp, A.E., 1993. A model for the motion of the Philippine Sea plate consistent with NUVEL-1 and geological data. *J. Geophys. Res.,* 98:17941–17948.

Shipboard Scientific Party, 1991. Site 808. *In* Taira, A., Hill, I., Firth, J., et al., *Proc. ODP, Init. Repts.,* 131: College Station, TX (Ocean Drilling Program), 71–269.

————, 2001a. Site 1173. *In* Moore, G.F., Taira, A., Klaus, A., et al., *Proc. ODP, Init. Repts.,* 190 [CD ROM]. Available from: Ocean Drilling Program, Texas A&M University, College Station TX 77845-9547, USA.

————, 2001b. Site 1174. *In* Moore, G., Taira, A., Klaus, A., et al., *Proc. ODP, Init. Repts.,* 190 [CD ROM]. Available from: Ocean Drilling Program, Texas A&M University, College Station TX 77845-9547, USA.

Suess, E., and Whiticar, M.J., 1989. Methane-derived CO_2 in pore fluids expelled from the Oregon subduction zone. *Palaeogeogr., Palaeoclimatol., Palaeoecol.,* 71:119–136.

Tada, R., and Iijima, A., 1983. Identification of mixtures of opaline silica phases and its implication for silica diagenesis. *In* Iijima A., Hein, J.R., and Siever, R. (Eds.), *Siliceous Deposits in the Pacific Region:* Amsterdam (Elsevier), 229–245.

Taira, A., Katto, J., Tashiro, M., Okamura, M., and Kodama, K., 1988. The Shimanto Belt in Shikoku, Japan: evolution of a Cretaceous to Miocene accretionary prism. *Mod. Geol.,* 12:5–46.

Vrolijk, P., Fisher, A., and Gieskes, J., 1991. Geochemical and geothermal evidence for fluid migration in the Barbados accretionary prism (ODP Leg 110). *Geophys. Res. Lett.,* 18:947–950.

Wang, K., Hyndman, R.D., and Yamano, M., 1995. Thermal regime of the Southwest Japan subduction zone: effects of age history of the subducting plate. *Tectonophysics,* 248:53–69.

Yamano, M., Foucher, J.-P., Kinoshita, M., Fisher, A., Hyndman, R.D., and ODP Leg 131 Shipboard Scientific Party, 1992. Heat flow and fluid flow regime in the western Nankai accretionary prism. *Earth Planet. Sci. Lett.,* 109:451–462.

TABLE CAPTION

Table T1. Leg 196 operations summary.

FIGURE CAPTIONS

Figure F1. Location map showing positions of Leg 190 and 196 sites. The red box outlines the location of the three-dimensional seismic survey. Yellow numbers indicate sites revisited during Leg 196. Depth contours are in kilometers.

Figure F2. Generalized depth section showing site locations and major structural features and provinces. This drawing is based on seismic reflection data from Hills et al. (unpubl. data). VE = vertical exaggeration. Seismic time section across Leg 196 Sites 1173 and 808 showing the transition from the Shikoku Basin to the imbricate thrust zone. The section is composed of a northwest-trending segment of seismic line 215 through Site 1173, with a diagonal transition to line 281 that passes near Sites 1174 and 808. CDP = common depth point.

Figure F3. Seismic time section across Leg 196 Sites 1173 and 808 showing the transition from the Shikoku Basin to the imbricate thrust zone. The section is composed of a northwest-trending segment of seismic line 215 through Site 1173, with a diagonal transition to line 281 that passes near Sites 1174 and 808. CDP = common depth point.

Figure F4. Seismic depth section across Leg 196 Sites 1173, 1174, and 808 (Hills et al., unpubl. data). The section is composed of a northwest-trending segment of seismic Line 215 through Site 1173, with a diagonal transition to Line 281 that passes near Sites 1174 and 808. VE = vertical exaggeration.

Figure F5. Site 1173 summary diagram that combines results of Legs 190 and 196. From left: depth-converted seismic reflection data, core recovery, core-based lithology and facies interpretation, bedding dip, pore water geochemistry, temperature-depth gradient, log resistivity, clay mineral content, and gamma ray log, core and log density, and core and log porosity (computed from the density log using core grain density values). VE = vertical exaggeration, CDP = common depth point, RAB = resistivity at the bit, SFLU = spherically focused resistivity measurement, XRD = X-ray diffraction, ACORK = advanced circulation obviation retrofit kit.

Figure F6. Site 808 summary diagram showing combined results of Legs 131 and 196. From left: depth-converted seismic reflection data, core-based facies interpretation, recovery, lithologic units and lithology, logging-while-drilling (LWD) gamma ray, core and LWD density, core and log porosity (computed from the density log using core grain density values), pore water chlorinity, fracture dip from LWD resistivity-at-the-bit (RAB) images, core *P*-wave velocities, and LWD resistivity. CDP = common depth point, ACORK = advanced circulation obviation retrofit kit.

Figure F7. RAB image of Hole 808I showing all interpreted fractures. Fractures are separated into conductive (blue) and resistive (red) fractures. Tadpoles show fractures as dip direction with respect to north and dip (0°–90°). Deformation intensifies significantly at the frontal thrust (389–414 mbsf), a fractured interval correlated with Leg 131, Site 808 core analysis (559–574 mbsf), and the décollement zone (~950 mbsf). The interval of continuous strong borehole breakouts is labeled between ~270 and ~530 mbsf, coincident with logging Unit 2 and bracketing the frontal thrust zone. Fracture orientations are dominantly northeast-southwest (dip directions: northwest-southeast) within the frontal thrust and 560-mbsf fractured interval but are more randomly oriented with depth. A north-south fracture orientation (east-west dip direction) is dominant within the décollement zone.

Figure F8. RAB image of breakouts (dark low-resistivity parallel lines down image) at 460–505 mbsf in Hole 808I showing images at 1-in (shallow), 3-in (medium), and 5-in (deep) penetration from the borehole. This image is ~100 m below the frontal thrust zone, close to the base of logging Unit 2. The breakouts indicate the orientation of the minimum horizontal compressive stress (σ_2) ~northeast-southwest, which is in good agreement with the plate convergence vector of ~310°–314° aligned with the maximum compressive stress, σ_1 (90° to σ_2).

Site 1173

Hole 1173B

Latitude: 32°14.6831'N
Longitude: 135°01.4845'E
Seafloor depth from rig floor (mbrf): 4801.9
Rig floor elevation above sea level (m): 10.8
Water depth (mbsl): 4791.1

Operation	Start date (2001)	Start time (local)	End date (2001)	End time (local)	Top depth (mbsf)	Bottom depth (mbsf)	Drilled (mbsf)	Time on hole (hr)	Time on hole (days)	Comments
Install reentry cone and 20-in casing	10-May	2:24	13-May	23:15	0	124.2	124.2	88.5	3.69	20-in casing shoe at 120.6 mbsf
LWD	13-May	23:15	17-May	21:35	124.2	737.1	612.9	94.3	3.93	
Open 9.875-in LWD hole to 17.5 in for ACORK	23-May	19:10	2-Jun	2:30	124.2	735.1	610.9	79.3	3.31	17.5-in hole extends to 732.1 mbsf
Assemble and drill in ACORK	2-Jun	2:30	10-Jun	4:45	—	—	—	194.2	8.09	ACORK extends from 0 to 727.10 mbsf; includes 58 hr DP transit back to site
RCB core below ACORK: Open basement hydrologic system to deepest monitoring zone	10-Jun	4:45	12-Jun	16:15	737.1	756.6	19.5	59.5	2.48	Three cores; 19.5 m cored; 5.19 m recovered (27%)
Install bridge plug inside ACORK	12-Jun	16:15	14-Jun	0:00	—	—	—	31.7	1.32	Bridge plug set at 466 mbsf; drill pipe broke off at ACORK head
Conduct camera survey of ACORK	29-Jun	4:00	29-Jun	22:15	—	—	—	18.3	0.76	
				Totals for Hole 1173B:			1367.5	565.8	23.58	

Hole 1173C

Latitude: 32°14.6978'N
Longitude: 135°01.4612'E
Seafloor depth from rig floor (mbrf): 4801.9
Rig floor elevation above sea level (m): 10.8
Water depth (mbsl): 4791.1

Operation	Start date (2001)	Start time (local)	End date (2001)	End time (local)	Top depth (mbsf)	Bottom depth (mbsf)	Drilled (mbsf)	Time on hole (hr)	Time on hole (days)	Comments
LWD	17-May	21:35	18-May	16:55	0	175.0	175.0	19.4	0.81	
				Totals for Hole 1173C:			175.0	19.4	0.81	
				Totals for Site 1173:			1542.5	585.2	24.4	

Table T1

Site 808

Hole 808H

Latitude:	32°21.2142'N
Longitude:	134°56.7009'E
Seafloor depth from rig floor (mbrf):	4686.0
Rig floor elevation above sea level (m):	10.9
Water depth (mbsl):	4675.1

Operation	Start date (2001)	Start time (local)	End date (2001)	End time (local)	Top depth (mbsf)	Bottom depth (mbsf)	Drilled (mbsf)	Time on hole (hr)	Time on hole (days)	Comments
Install reentry cone and 20-in casing	18-May	19:37	20-May	19:10	0	126.7	126.7	47.5	1.98	Mud motor failed; pulled out of hole; hole abandoned
				Totals for Hole 808H:			126.7	47.5	1.98	

Hole 808I

Latitude:	32°21.2145'N
Longitude:	134°56.7003'E
Seafloor depth from rig floor (mbrf):	4686.0
Rig floor elevation above sea level (m):	10.9
Water depth (mbsl):	4675.1

Operation	Start date (2001)	Start time (local)	End date (2001)	End time (local)	Top depth (mbsf)	Bottom depth (mbsf)	Drilled (mbsf)	Time on hole (hr)	Time on hole (days)	Comments
Install reentry cone and 20-in casing	20-May	19:10	22-May	11:30	0	160.1	160.14	40.3	1.68	20-in casing shoe at 156.6 mbsf
LWD	22-May	11:30	27-May	17:10	160.1	1057.6	897.4	125.7	5.24	Unable to penetrate past 1057.6 mbsf
Open 9.875-in LWD hole to 17.5 in for ACORK	14-Jun	1:30	18-May	15:55	160.1	975.3	815.2	110.4	4.60	
Assemble and drill in ACORK	18-Jun	15:55	28-May	19:45	—	—	—	243.8	10.16	964-m-long ACORK could only be drilled in to 927 mbsf; time on hole includes 17-hr DP transit back to site
				Totals for Hole 808I:			1872.7	520.2	21.68	
				Totals for Site 808:			1999.4	615.3	23.66	
				Totals for Leg 196:			3541.9	1153.0	48.05	

Note: LWD = logging while drilling, ACORK = advanced circulation obviation retrofit kit, DP = dynamic positioning, RCB = rotary core barrel.

Table T1 (continued)

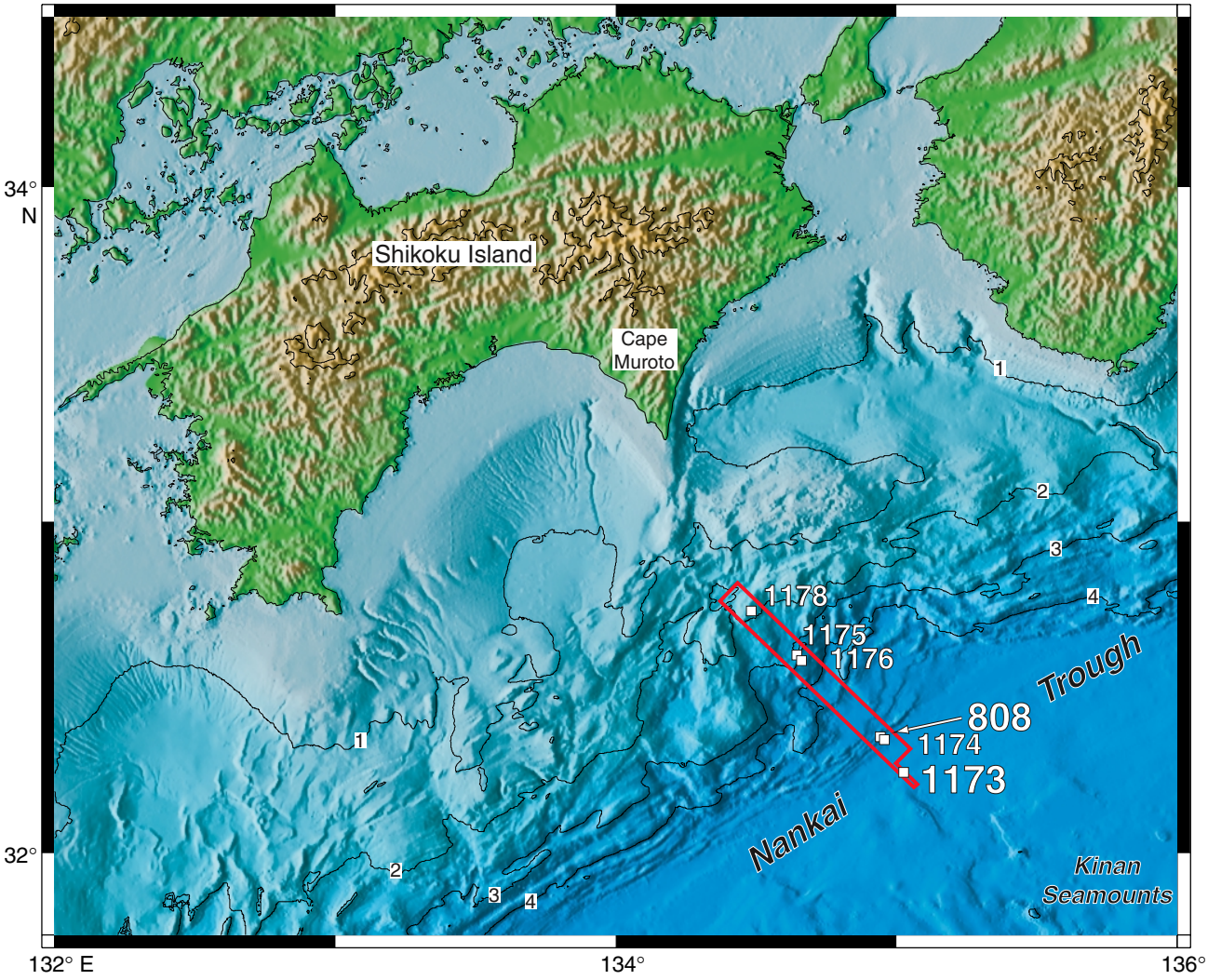
34° N
32°
132° E
134°
136°
Shikoku Island
Cape Muroto
1178
1175
1176
808
1174
1173
Trough
Nankai
Kinan Seamounts
1
2
3
4

Figure F1

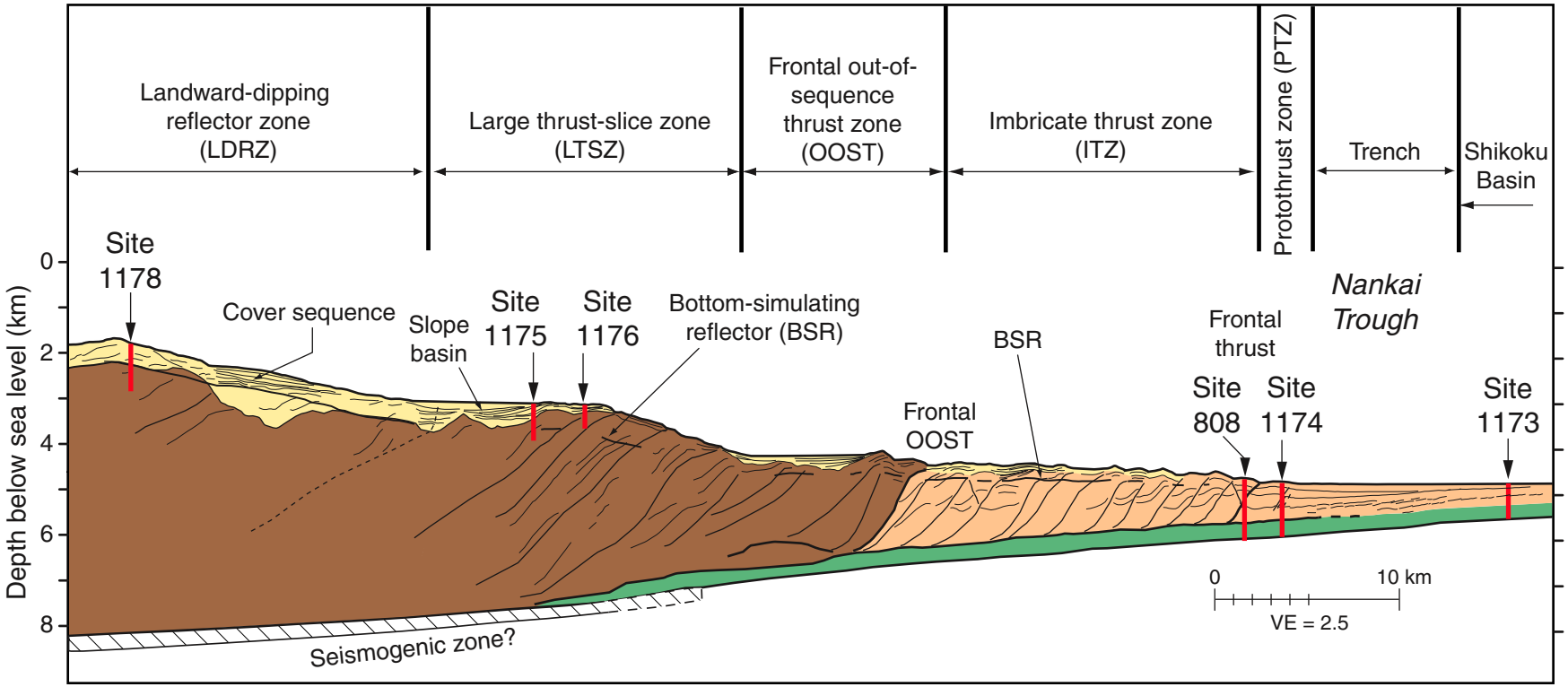
Landward-dipping reflector zone (LDRZ)
Large thrust-slice zone (LTSZ)
Frontal out-of-sequence thrust zone (OOST)
Imbricate thrust zone (ITZ)
Prototrust zone (PTZ)
Trench
Shikoku Basin
Site 1178
Cover sequence
Slope basin
Site 1175
Site 1176
Bottom-simulating reflector (BSR)
BSR
Frontal OOST
Frontal thrust
Nankai Trough
Site 808
Site 1174
Site 1173
Depth below sea level (km)
0
2
4
6
8
0
10 km
VE = 2.5
Seismogenic zone?

Figure F2

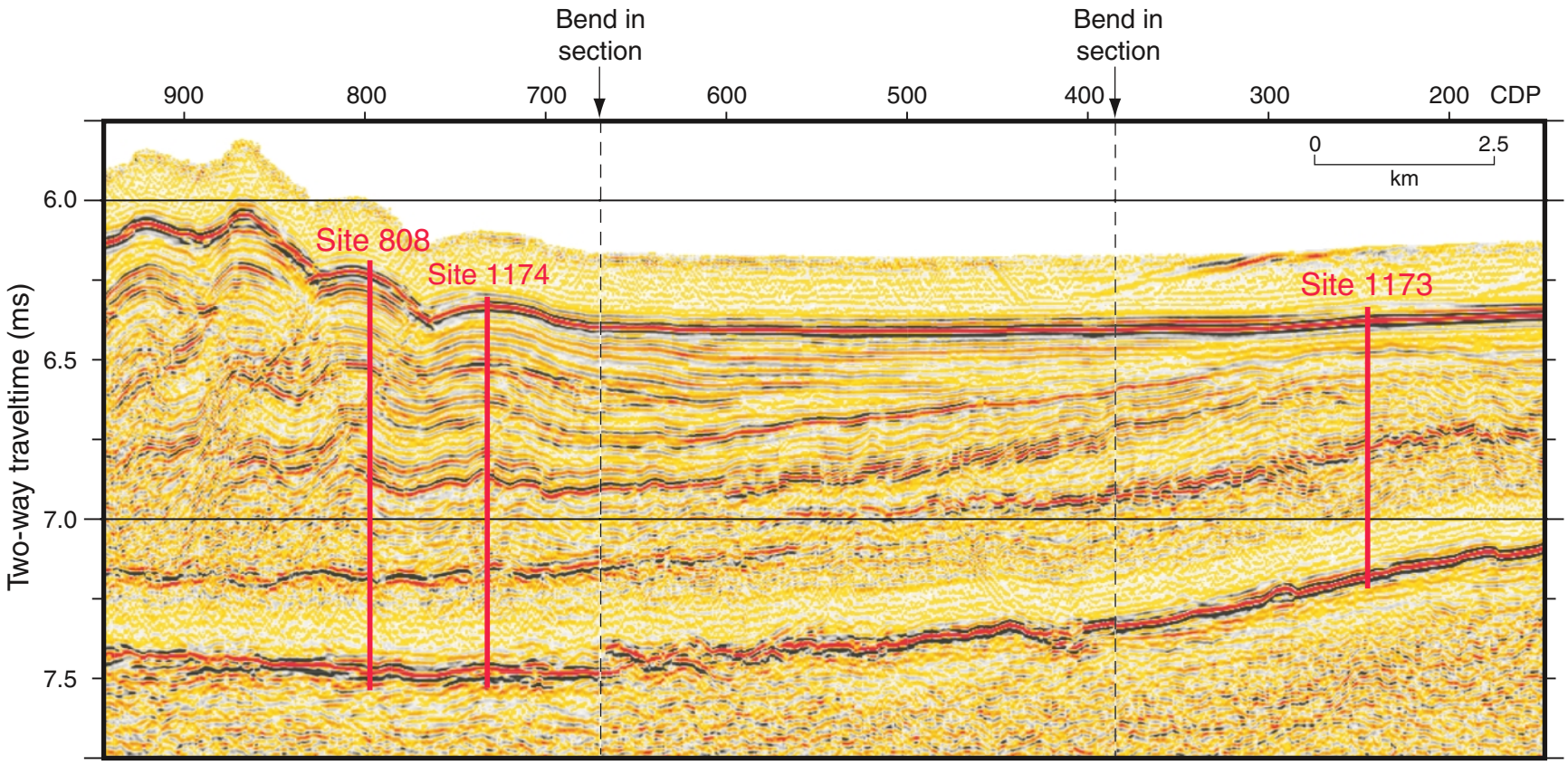
Bend in section
Bend in section
900
800
700
600
500
400
300
200
CDP
0
2.5
km
6.0
6.5
7.0
7.5
Two-way traveltime (ms)
Site 808
Site 1174
Site 1173

Figure F3

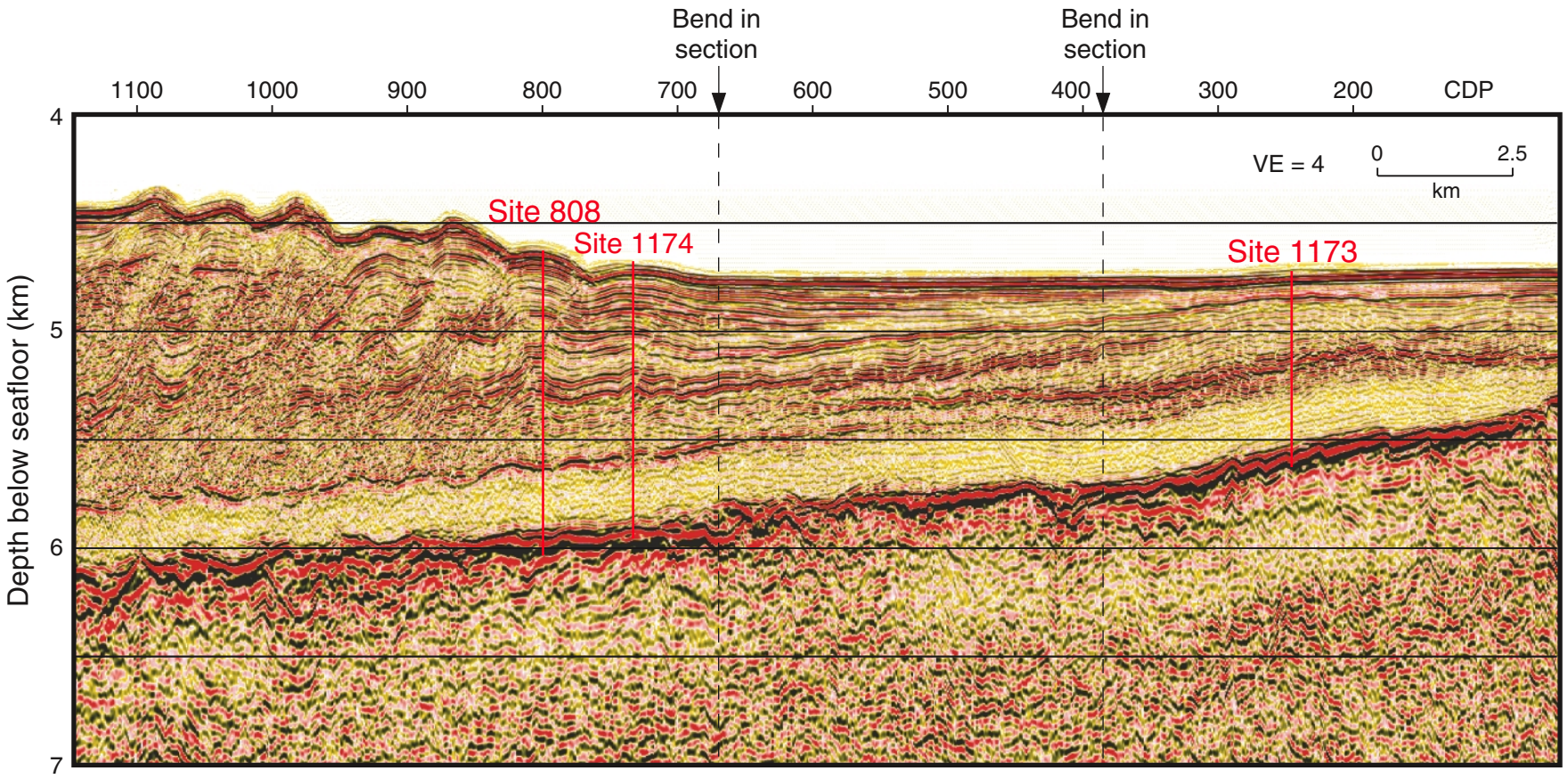
Bend in section
Bend in section
1100
1000
900
800
700
600
500
400
300
200
CDP
4
5
6
7
Depth below seafloor (km)
VE = 4
0
2.5
km
Site 808
Site 1174
Site 1173

Figure F4

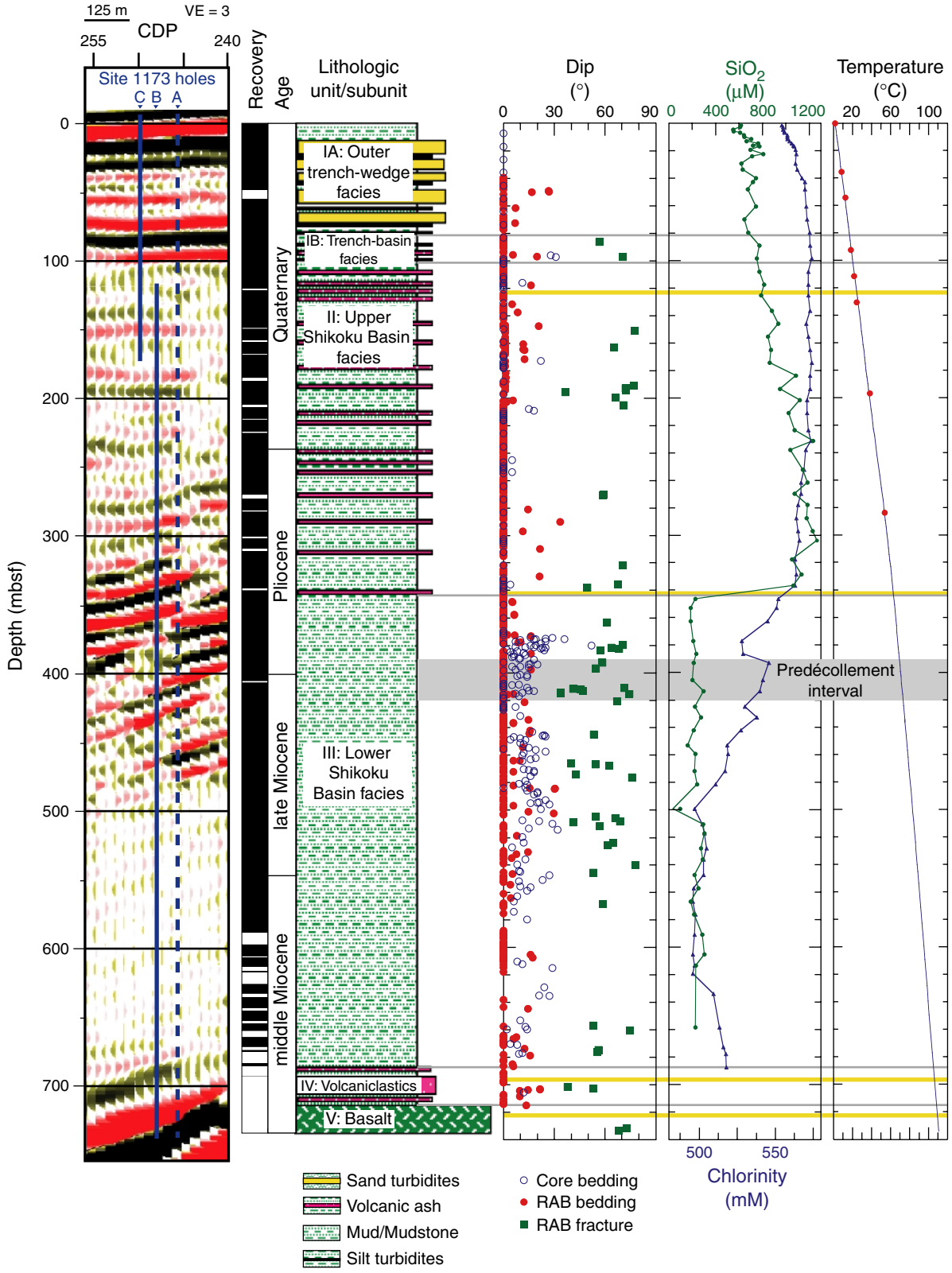
125 m
VE = 3
CDP
255
240
Site 1173 holes
C B A
Recovery
Age
Lithologic unit/subunit
Dip (°)
SiO2 (µM)
Temperature (°C)
Depth (mbsf)
Quaternary
Pliocene
late Miocene
middle Miocene
IA: Outer trench-wedge facies
IB: Trench-basin facies
II: Upper Shikoku Basin facies
III: Lower Shikoku Basin facies
IV: Volcaniclastics
V: Basalt
Predécollement interval
Chlorinity (mM)
Sand turbidites
Volcanic ash
Mud/Mudstone
Silt turbidites
Core bedding
RAB bedding
RAB fracture

Figure F5

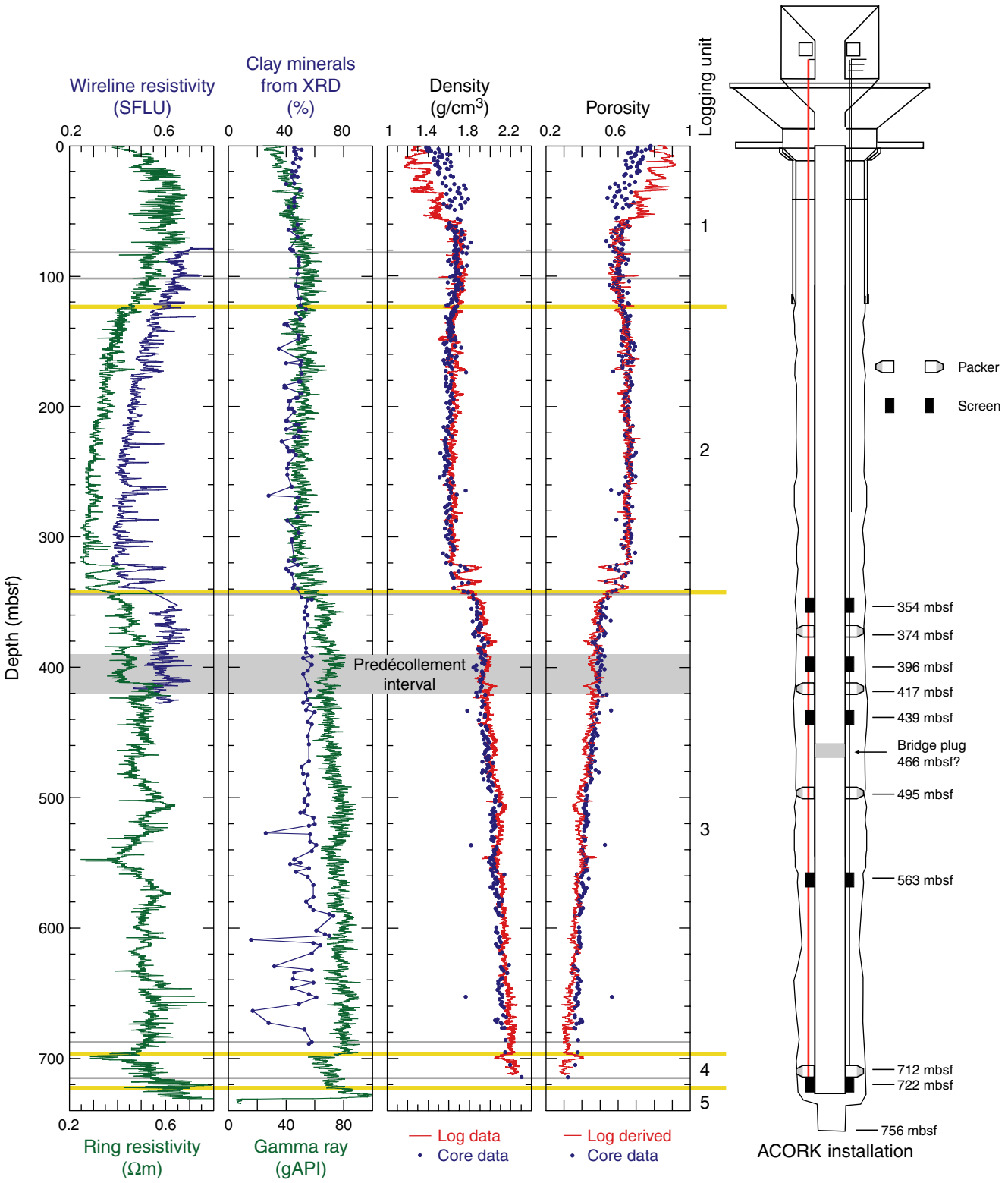

Figure F5 (continued)

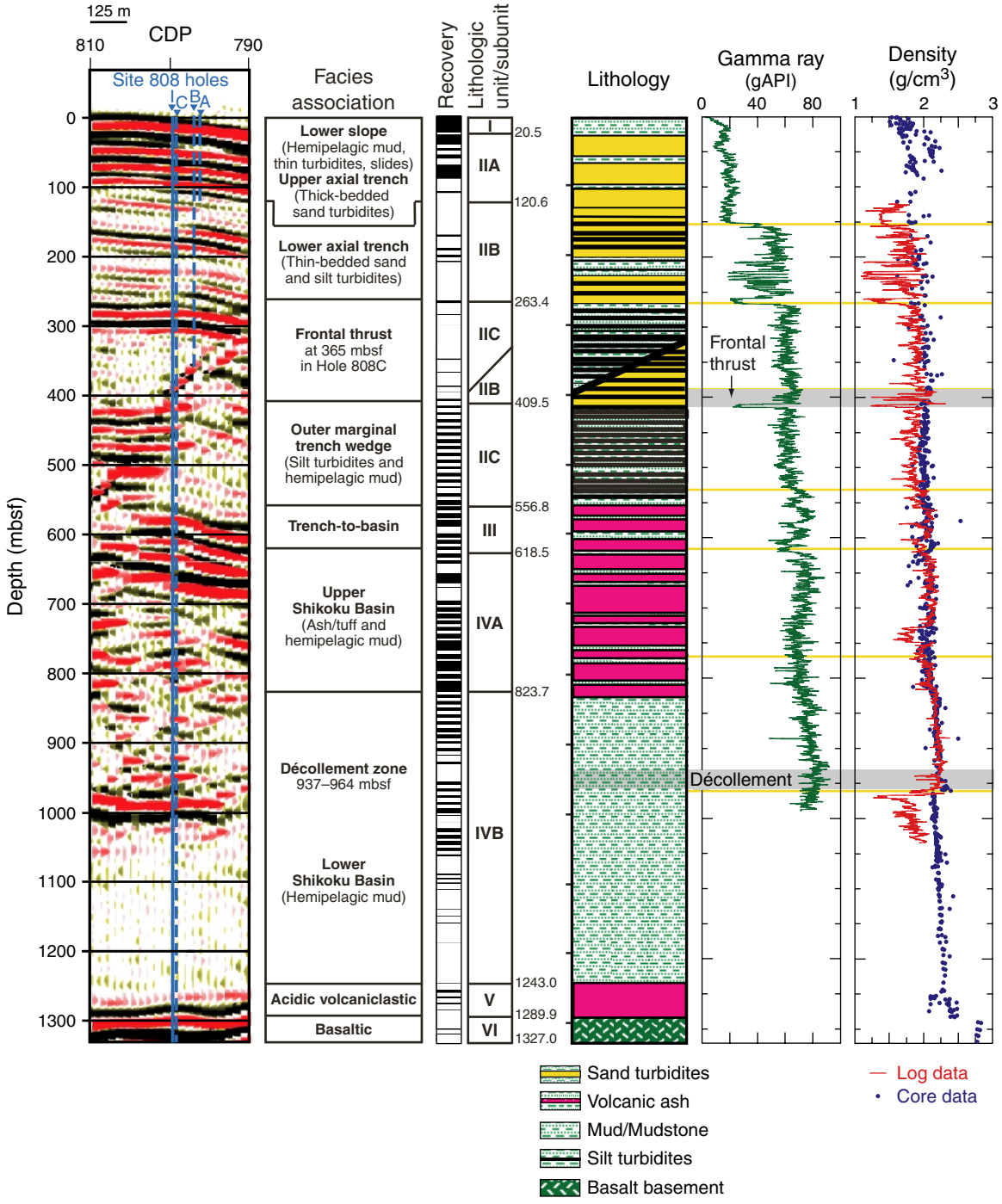
125 m
CDP
810
790
Site 808 holes
C B A
Depth (mbsf)
0
100
200
300
400
500
600
700
800
900
1000
1100
1200
1300
Facies association
Lower slope
(Hemipelagic mud, thin turbidites, slides)
Upper axial trench
(Thick-bedded sand turbidites)
Lower axial trench
(Thin-bedded sand and silt turbidites)
Frontal thrust
at 365 mbsf
in Hole 808C
Outer marginal trench wedge
(Silt turbidites and hemipelagic mud)
Trench-to-basin
Upper Shikoku Basin
(Ash/tuff and hemipelagic mud)
Décollement zone
937–964 mbsf
Lower Shikoku Basin
(Hemipelagic mud)
Acidic volcaniclastic
Basaltic
Recovery
Lithologic unit/subunit
I
IIA
IIB
IIC
IIB
IIC
III
IVA
IVB
V
VI
20.5
120.6
263.4
409.5
556.8
618.5
823.7
1243.0
1289.9
1327.0
Lithology
Gamma ray (gAPI)
0
40
80
Density (g/cm3)
1
2
3
Frontal thrust
Décollement
Sand turbidites
Volcanic ash
Mud/Mudstone
Silt turbidites
Basalt basement
Log data
Core data

Figure F6

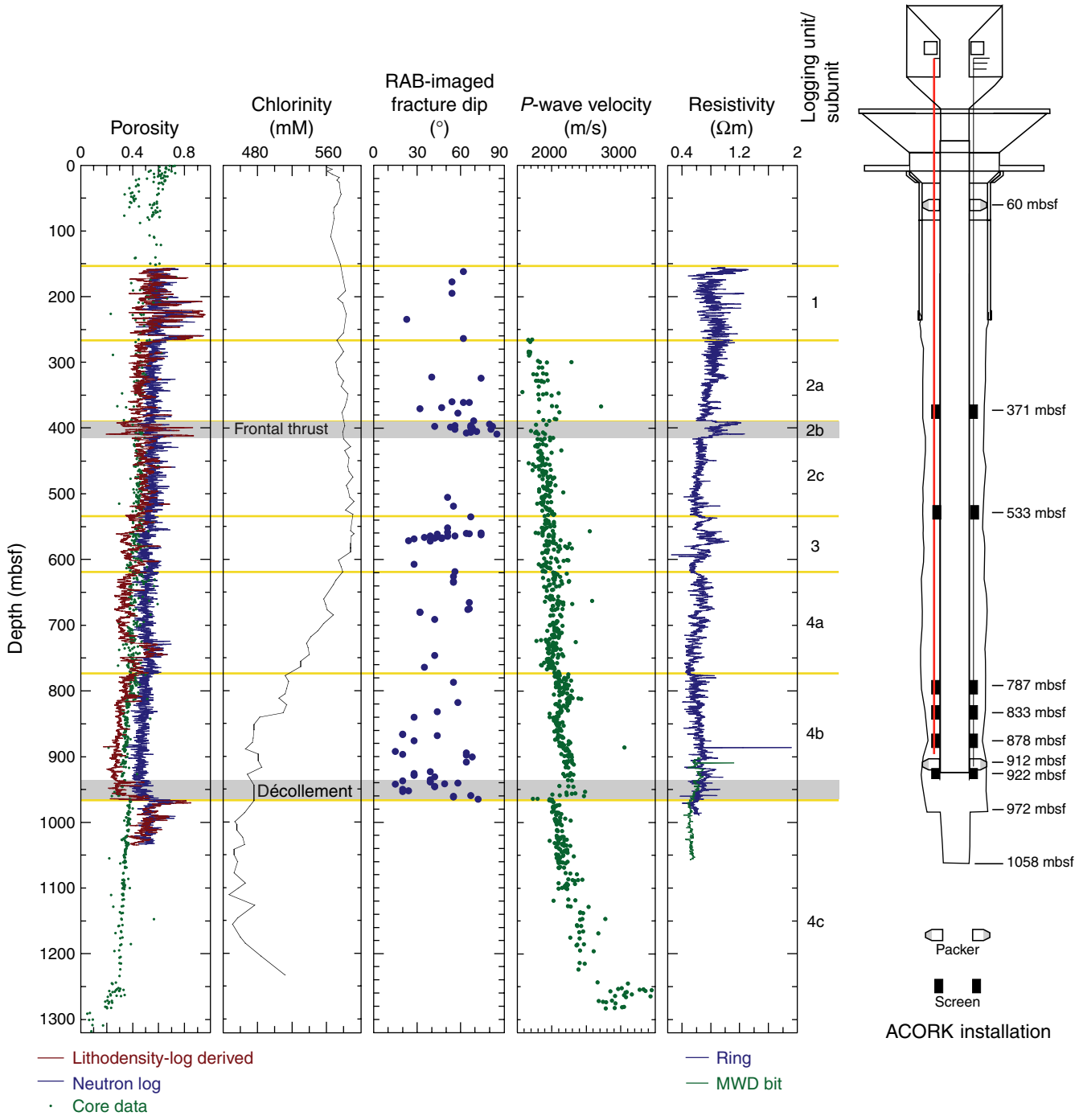

Figure F6 (continued)

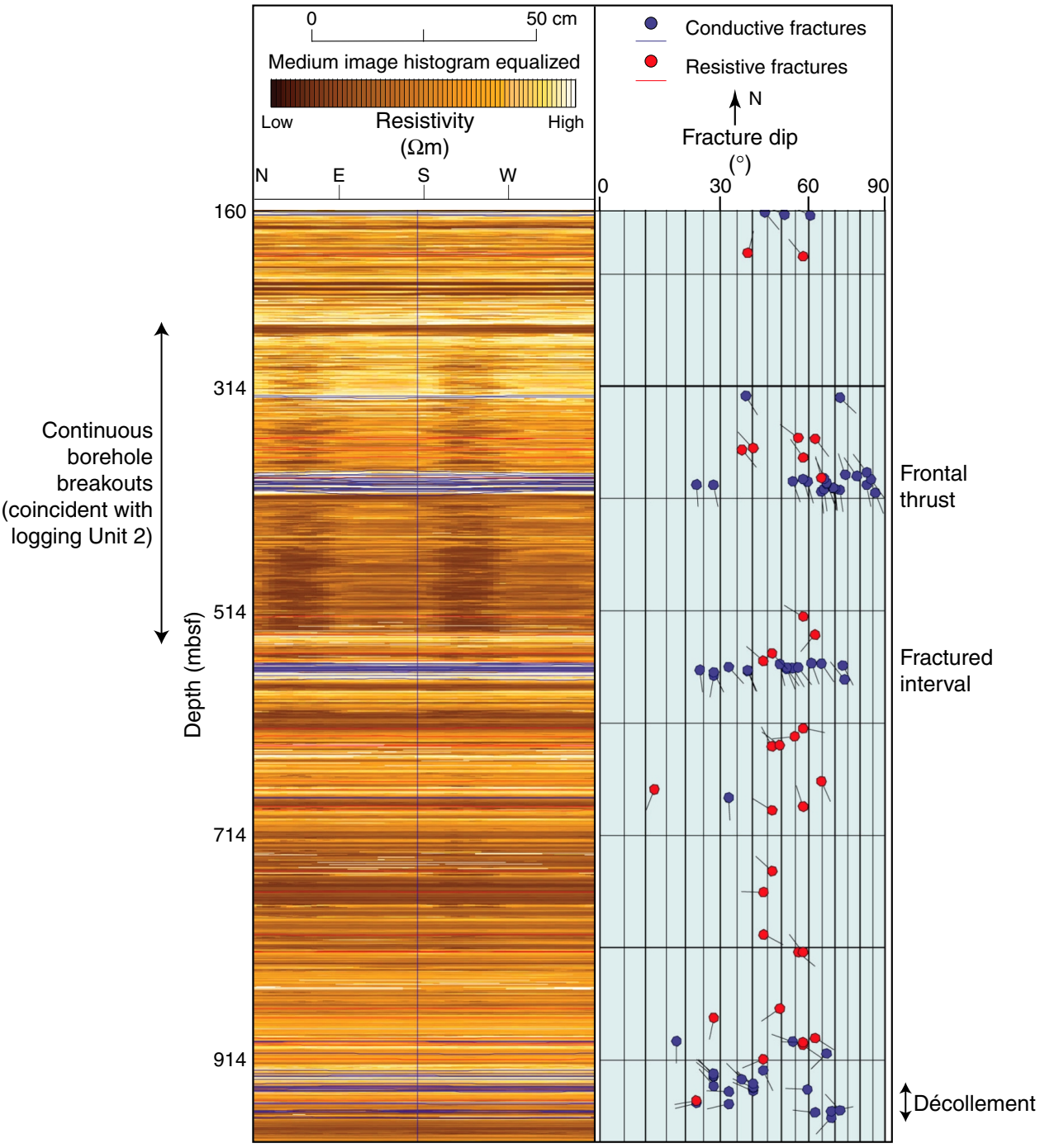
0
50 cm
Medium image histogram equalized
Low
Resistivity
(Ωm)
High
N
E
S
W
Conductive fractures
Resistive fractures
N
Fracture dip
(°)
0
30
60
90
160
314
514
714
914
Depth (mbsf)
Continuous borehole breakouts (coincident with logging Unit 2)
Frontal thrust
Fractured interval
Décollement

Figure F7

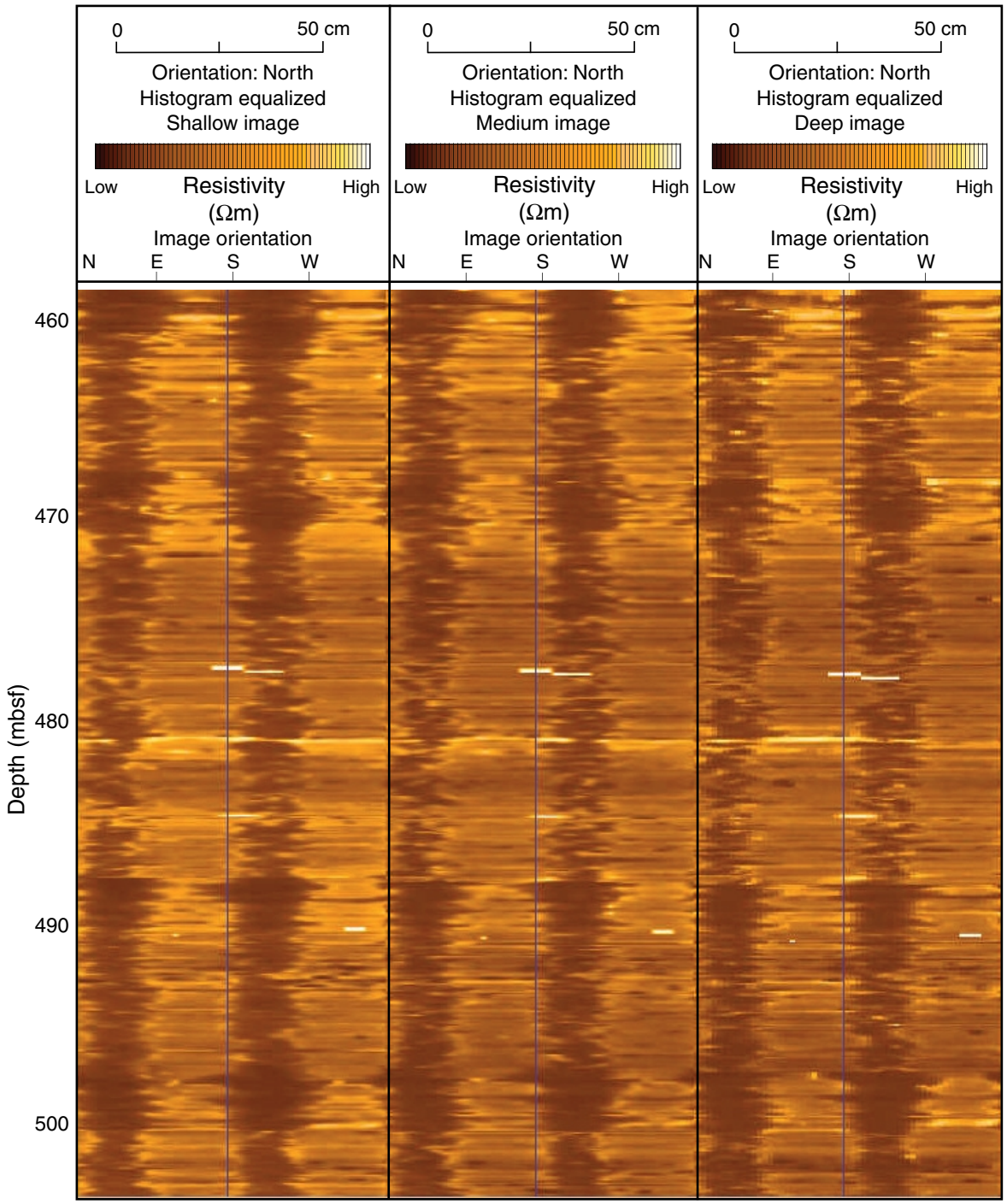
0
50 cm
Orientation: North
Histogram equalized
Shallow image
Low
Resistivity
(Ωm)
High
Image orientation
N
E
S
W
Medium image
Deep image
Depth (mbsf)
460
470
480
490
500

Figure F8